

RESEARCH ARTICLE

Assessing reliability of precipitation data over the Mekong River Basin: A comparison of ground-based, satellite, and reanalysis datasets

Aifang Chen¹ | Deliang Chen^{1,2,3}  | Cesar Azorin-Molina¹ 

¹Regional Climate Group, Department of Earth Sciences, University of Gothenburg, Gothenburg, Sweden

²Key Laboratory of Tibetan Environment Changes and Land Surface Processes, Institute of Tibetan Plateau Research, Chinese Academy of Sciences, Beijing, China

³CAS Center for Excellence in Tibetan Plateau Earth Sciences, Beijing, China

Correspondence

Deliang Chen, Regional Climate Group, Department of Earth Sciences, University of Gothenburg, Box 460, 405 30 Gothenburg, Sweden.

Email: deliang@gvc.gu.se

Funding information

Strategic Priority Research Program of Chinese Academy of Sciences, Grant/Award Number: XDA20060401; China Scholarship Council; European Union's Horizon 2020 research and innovation programme under the Marie Skłodowska-Curie grant agreement, Grant/Award Number: 703733; National Natural Science Foundation of China, Grant/Award Number: 91537210; Swedish Foundation for International Cooperation in Research and Higher Education, Grant/Award Number: CH2015-6226

Accurate precipitation data are the basis for hydro-climatological studies. As a highly populated river basin, with the biggest inland fishery in Southeast Asia, freshwater dynamics is extremely important for the Mekong River Basin (MB). This study focuses on evaluating the reliability of existing gridded precipitation datasets both from satellite and reanalysis, with a ground observations-based gridded precipitation dataset as the reference. Two satellite products (Tropical Rainfall Measuring Mission [TRMM] and the Precipitation Estimation from Remote Sensing Information using an Artificial Neural Network—Climate Data Record [PERSIANN-CDR]), as well as three reanalysis products (Modern-Era Retrospective analysis for Research and Applications [MERRA2], the European Centre for Medium-Range Weather Forecasts interim reanalysis [ERA-Interim], and the Climate Forecast System Reanalysis [CFSR]) were compared with the Asian Precipitation—Highly Resolved Observational Data Integration Towards Evaluation of Water Resources (APHRODITE) over the MB. The APHRODITE was chosen as the reference for the comparison because it was developed based on ground observations and has also been selected as reference data in previous studies. Results show that most of the assessed datasets are able to capture the major climatological characteristics of precipitation in the MB for the 10-year study period (1998–2007). Generally, both satellite data (TRMM and PERSIANN-CDR) show higher reliability than reanalysis products at both spatial and temporal scales across the MB, with the TRMM outperforming when compared to the PERSIANN-CDR. For the reanalysis products, MERRA2 is more reliable in terms of temporal variability, but with some underestimation of precipitation. The other two reanalysis products CFSR and ERA-Interim are relatively unreliable due to large overestimations. CFSR is better positioned to capture the spatial variability of precipitation, while ERA-Interim shows inconsistent spatial patterns but more realistically resembles the daily precipitation probability. These findings have practical implications for future hydro-climatological studies.

KEYWORDS

Mekong River Basin, precipitation evaluation, rain gauge observations, reanalysis data, satellite data

1 | INTRODUCTION

Precipitation plays a key role in the global hydrological cycle (Pascale *et al.*, 2015), combining both processes in

land-surface (i.e., surface runoff, infiltration, soil moisture, and groundwater) and atmosphere (i.e., cloud, evaporation, and precipitation) (Su and Hao, 2001; Andersson *et al.*, 2005). According to the Clausius–Clapeyron relation, warm

air is expected to hold more moisture (Held and Soden, 2000; Bengtsson, 2010) and the increasing saturation vapour pressure along with global warming could result in the variability of precipitation (Ramanathan, 2001). Unlike air temperature, precipitation is of large spatial heterogeneity, strongly controlled by atmospheric circulation, land cover, and local topography (Decker *et al.*, 2012). Particularly, it receives increasing disturbances from human activity; for example, water consumption and water transportation through artificial river canals, dams, and reservoirs. Therefore, long-term precipitation variability is one of the highest concerns among climate scientists (Pascale *et al.*, 2015) and society at large. Under global climate change, no agreements on precipitation changes on the global scale have yet been reached (IPCC, 2013; Wang *et al.*, 2018). However, adequate observation and exploration could lay the foundations for a better understanding of past global precipitation patterns, and thus contribute to improved predictions which could lead to potential mitigations and adaptations in the future (Tang *et al.*, 2009; IPCC, 2013).

As the primary freshwater source, precipitation is vital for the sustainable development of people inhabiting in the Mekong River Basin (MB). On account of the ecosystem services provided by the Mekong River, a population of over 60 million live in the Lower MB (LMB) which supports one of the world's largest inland fisheries (Pech and Sunada, 2008; Ziv *et al.*, 2012; Piesse, 2016). The climate in the MB is very complex, with high spatio-temporal variability (MRC, 2010). Additionally, owing to the changing hydrological processes induced by climate change (Hoang *et al.*, 2016), water-related extreme events, especially droughts and floods, have shown increasing trends in the MB since the 20th century, affecting agriculture, fishery, water resources, and ecosystems (Delgado *et al.*, 2010; Hoang *et al.*, 2016). Although rain gauges can directly measure precipitation that reaches the ground surface (Ashouri *et al.*, 2015), the available rain gauges are sparsely and unevenly distributed across the MB (Wang *et al.*, 2016), which is not enough to thoroughly monitor the spatial features of precipitation over the region. This is because many gaps and discontinuities exist as the result of conflicts among the riparian countries of the LMB during the second half of the 20th century (Lutz *et al.*, 2014). Accordingly, to better explore and understand the changing hydroclimate across the MB, it is crucial to assess the reliability of gridded precipitation datasets.

With advances in technology and science, both satellite and reanalysis methods offer precipitation data with fine spatio-temporal resolutions, especially in far-remote areas with sparse in situ precipitation networks. Generally, satellite observation provides an indirect method to estimate precipitation with consistent spatial continuity and relatively high temporal frequency (Tang *et al.*, 2009; 2010; Nasrollahi *et al.*, 2013). Moreover, reanalysis methods offer precipitation estimations by assimilating all available data into a

background forecast physical model (Wong *et al.*, 2017). Because a series of satellite and reanalysis gridded precipitation datasets have been released by many international institutions over recent decades (e.g., Moderate Resolution Imaging Spectroradiometer by the National Aeronautics and Space Administration [NASA], and ERA-Interim by the European Centre for Medium-Range Weather Forecasts [ECMWF]), their great efforts in continuously upgrading data methodologies have brought state-of-the-art precipitation datasets (Decker *et al.*, 2012). Despite this advancement, these available gridded precipitation datasets are produced by unique remote sensors and numerical models, therefore the quality and quantity of observational data used in the assimilation processes result in discrepancies among them (Decker *et al.*, 2012; Wang and Zeng, 2012). Henceforth, the quality of the gridded precipitation datasets must be evaluated before further study on Climatology and Hydrology.

Previous studies have evaluated the performance of satellite and reanalysis precipitation datasets at various spatial scales such as the global (i.e., (Decker *et al.*, 2012; Lorenz and Kunstmann, 2012); Gebregiorgis and Hossain, 2015), European (Kidd *et al.*, 2012), Asian (Zhou *et al.*, 2008; Rana *et al.*, 2015; Ceglar *et al.*, 2017), African (Koutsouris *et al.*, 2016), North American (Kirstetter *et al.*, 2013; Seyyedi *et al.*, 2015; Wong *et al.*, 2017), South American (Salio *et al.*, 2015), and Tropical Pacific basin (Chen *et al.*, 2013). Table 1 summarizes a review of some studies dealing with the evaluation of precipitation from ground-based, satellite, and reanalysis products. Overall, precipitation datasets produced by different institutions show a wide array of performance on various spatio-temporal scales which can be attributed to the diversity of environmental conditions (Berg *et al.*, 2006). Specifically, satellite precipitation products generally capture rainfall spatio-temporal variability better than the reanalysis and land data assimilation products, with reference gauge data (Rana *et al.*, 2015; Seyyedi *et al.*, 2015; Tan *et al.*, 2017). However, satellite data tend to underestimate precipitation in the cold season (Kidd *et al.*, 2012; Huang *et al.*, 2016a). Among the satellite data, Tropical Rainfall Measuring Mission (TRMM) products present overall good performance (Zhou *et al.*, 2008; Yamamoto *et al.*, 2011; Salio *et al.*, 2015). TRMM post-real-time research product version 7, 3B42v7 exhibits higher performance in comparison to its predecessor, 3B42v6 (Chen *et al.*, 2013; Kirstetter *et al.*, 2013; Rana *et al.*, 2015). As for the reanalysis data, ERA-Interim, Climate Forecast System Reanalysis (CFSR), and Modern-Era Retrospective analysis for Research and Applications (MERRA) also capture the principal precipitation variability well (Wang and Zeng, 2012; Huang *et al.*, 2016b; Koutsouris *et al.*, 2016).

For the MB, there are few regional assessments of precipitation dataset performance. For instance, in a further trend analysis, Lutz *et al.* (2014) evaluated four selected

TABLE 1 A review of precipitation evaluations among ground-based, satellite, and reanalysis products^a

Study number	Source	Reference data	Investigated data	Location	Period	Study details: data performance
1	Decker <i>et al.</i> (2012)	FLUXNET	CFSR, ERA-40, ERA-Interim, GLDAS, MERRA	Globe	1991–2006	Both GLDAS and ERA-Interim perform better on the precipitation variability than CFSR, ERA-40, and MERRA.
2	Gebregiorgis and Hossain (2015)	APHRODITE, NEXRAD-IV, CPC, ECAD E-OBS, TRMM2A25-PR	CMORPH, PERSIANN-CCS, TRMM3B42RT	Globe	2003–2007	The error variance of satellite data is highly correlated to observations, and the quantitative picture of satellite precipitation error over ungauged regions can be discerned even in the absence of ground truth data.
3	Lorenz and Kunstmann (2012)	CPC, CRU, GPCC, GPCC, UDEL	CFSR, ERA-Interim, MERRA	Globe	1989–2006	Reanalysis datasets are highly uncertain in terms of spatial variability and total amount. The largest discrepancies occur in the summer months of the respective hemisphere. The highest differences can be found over tropical Southeast Asia.
4	Kidd <i>et al.</i> (2012)	ECMWF, GPCC, GPI, surface radar, UK national hourly gauge data	CMORPH, NRLBLD, PERSIANN, TRMM3B42RT	Europe (Northwest Europe)	March 2005–February 2011	All the satellite data underestimate precipitation over Northwest Europe in all seasons, with poorer statistics during the winter.
5	Tanarhte <i>et al.</i> (2012)	Ensemble reference data	APHRODITE, CPC, CRU, ECAD E-OBS, GPCC, UDEL	The Mediterranean and the Middle East	1961–2000	All datasets represent the overall spatial features partly with biases.
6	Chen <i>et al.</i> (2013)	PACRAIN (gauge data)	TRMM3B42v6, TRMM3B42v7	Tropical Pacific Basin	1998–2010	TRMM 3B42v7 has been proved to be good at detecting intense TC rainfall and is also of higher performance when compared with TRMM 3B42v6
7	Higgins <i>et al.</i> (2010)	CPC	CFSR, NCEP1, NCEP2	North America (the United States)	1979–2006	The CFSR has been improved compared to NCEP1 and NCEP2. However, it is not sufficient to eliminate the bias (at least over the conterminous United States).
8	Kirsletter <i>et al.</i> (2013)	NOAA/NSL's ground radar-based National Mosaic and QPE system (NMQ/Q2)	TRMM2A25PRv6, TRMM2A25PRv7	North America (the southern conterminous United States)	March–May 2011	TRMM3B42v7 is in closer agreement with the reference rainfall compared to TRMM3B42v6.
9	Seyyedi <i>et al.</i> (2015)	The NCEP stage IV radar-rainfall product	GLDAS, TRMM3B42v7	North America (Mid-latitude basin in Northeastern United States)	2002–2011	TRMM3B42v7 exhibits significantly better error statistics compared to the GLDAS.
10	Wong <i>et al.</i> (2017)	AHCCD	ANUSPLIN, CaPA, NARR, NA-CORDEX, PCIC, PRINCETON, WFDEI (CRU), WFDEI (GPCC)	North America (Canada)	1979–2012	Most of the datasets were relatively skilful in central Canada.
11	Salio <i>et al.</i> (2015)	Gauge data (5,414 stations)	CMORPH, CoSch, HYDRO, TRMM3B42v6, TRMM3B42v7, TRMM3B42RT	South America (Southern South America)	December 2008–November 2010	The performance of satellite data improves in the “blended” estimates by including microwave observations and surface observations in the adjustments; that is, TRMM 3B42 V6, V7, and CoSch. However, large overestimations are detectable in CMORPH (extreme values over plains).

TABLE 1 (Continued)

Study number	Source	Reference data	Investigated data	Location	Period	Study details: data performance
12	Koutsouris <i>et al.</i> (2016)	TRMM3B42v7	CFSR, CMORPH, CRU, ERA-Interim, GPCC, MERRA, TRMM3B42v7, UDEL	Africa (Kilombero Valley, Tanzania)	1998–2010	All gridded precipitation data well represent the principal seasonality of the climatology. However, the intraseasonal variability and the spatial precipitation patterns were not as well-represented. The ensemble mean and GPCC has the best performance with regard to the analysis of the time series while CMORPH and GPCC have the best performance with regard to the spatial pattern analysis.
13	Alijaniyan <i>et al.</i> (2017)	Gauge data (958 stations)	CMORPH, MSWEP, PERSIANN, PERSIANN-CDR, TRMM3B42v6	Asia (Iran)	2003–2012	MSWEP has the highest CC, followed by TRMM3B42v6 and PERSIANN-CDR at the daily timescale. They performed well to distinguish rain from no-rain conditions, whereas for higher rainfall rates, PERSIANN-CDR outperforms the other satellite rainfall estimates.
14	Sidike <i>et al.</i> (2016)	Gauge data	APHRODITE, CRU, PRINCETON	Asia (Amu Darya River Basin)	1965–2007	The APHRODITE provides the highest accuracy, followed by the CRU NCEP reanalysis data and PRINCETON.
15	Yamamoto <i>et al.</i> (2011)	Gauge data (S-AWS site)	CMORPH, GSMaP, PERSIANN, TRMM3B42v6	Asia (Khumb region, Nepal)	1998–2004	TRMM3B42v6 corresponds to monthly mean precipitation in S-AWS throughout the year. All the products except for GSMaP show an increase in precipitation from late evening to midnight, consistent with S-AWS.
16	Ceglar <i>et al.</i> (2017)	APHRODITE, CHIRPS	AgMERRA, ERA-Interim, ERA-Interim/Land, JRA-55	Monsoon Asia	1981–2007	Remarkable differences between the APHRODITE and CHIRPS observational datasets as well as between these datasets and the reanalysis (ERA-Interim, ERA-Interim/Land, AgMERRA, and JRA-55)
17	Huang <i>et al.</i> (2016b)	CMAP, GPCP, Gauge data (from China)	ERA-Interim, JRA-25, MERRA, NCEP1, NCEP2	East Asia	1979–2012	MERRA and ERA-Interim have better skills in reproducing the climatology and interannual variability of the East Asian summer monsoon precipitation than NCEP1, NCEP2, and JRA-25
18	Sohn <i>et al.</i> (2012)	APHRODITE	CAMS-OPI, CMAP, ERA40, GPCP, JRA-25, NCEP2	East Asia	1979–2001	All reanalyses correlate well with APHRODITE data at monthly, seasonal, and annual scales; the performance of JRA-25 is the best for monitoring precipitation variations in East Asia. CAMS-OPI is found to be reliable for monitoring large-scale precipitation variations over the East Asian sector.
19	Rana <i>et al.</i> (2015)	APHRODITE	CFSR, CPC, ERA-Interim, GPCP, TRMM3B42v6, TRMM3B42v7,	South Asia (Indian subcontinent)	1997/98–2006/07	CPC and the satellite-derived precipitation products (GPCP, TRMM 3B42 v6, v7) capture the summer monsoon rainfall variability better than CFSR and ERA-Interim. Similar conclusions are drawn for the post-monsoon season, with the exception of 3B42 v7. Over mountainous regions, 3B42-V7 shows an appreciable improvement over 3B42 v6 and other gauge-based precipitation products.

TABLE 1 (Continued)

Study number	Source	Reference data	Investigated data	Location	Period	Study details: data performance
20	Tan <i>et al.</i> (2017)	Gauge data	APHRODITE, CFSR, PERSIANN-CDR	Southeast Asia (southern Peninsular Malaysia)	1983–2007	The APHRODITE data perform the best in precipitation estimation, followed by the PERSIANN-CDR and NCEP-CFSR datasets. The APHRODITE and PERSIANN-CDR data often underestimate the extreme precipitation and streamflow, while the NCEP-CFSR data produce dramatic overestimations.
21	Huang <i>et al.</i> (2016)	Gauge data (2,479 stations)	CMORPH, PERSIANN, TRMM3B41RTv7, TRMM3B42RTv7, TRMM3B42v7	China	2000–2014	Satellite precipitation datasets (CMORPH, PERSIANN, TRMM 3B42 RTv7, TRMM3B42RTv7, and TRMM3B42V7) generally capture the overall spatio-temporal variation of precipitation over China with a relatively better ability during warm seasons than in cold seasons, as well as over humid regions than arid and alpine regions, respectively.
22	Zhao <i>et al.</i> (2017)	Gauge data	TRMM3B42v7, TRMM3B42 RTv7	China (Southwestern China)	2000–2009	TRMM 3B42v7 shows higher CC with gauge data than TRMM3B42RTv7 in the Nantou River Basin. Both TRMM products increase with longer time-aggregated data; and the detection capability of daily values are enhanced by augmentation with daily precipitation rates.
23	Zhou <i>et al.</i> (2008)	Gauge data (626 stations)	PERSIANN, TRMM3B42	China	2000–2004	The TRMM 3B42 has a better resemblance with rain gauge observations in terms of both the pattern correlation and RMSE. The satellite products overestimate rainfall frequency but underestimate its intensity.
24	Gao and Liu (2013)	Gauge data (166 stations)	CMORPH, PERSIANN, TRMM3B42v6, TRMM3B42RTv6	Tibetan Plateau	2004–2009	TRMM3B42v6 and CMORPH show overall better performance than PERSIANN and TRMMRT, with higher CC and lower RMSEs.
25	Wang and Zeng (2012)	Gauge data (63 stations in 1992–2001, 9 stations in 2002–2004)	CFSR, ERA-40, ERA-Interim, GLDAS, MERRA, NCEP1,	Tibetan Plateau	1992–2004	GLDAS has the best overall performance in both daily and monthly precipitation, while ERA-40 and MERRA have the highest CC for daily and monthly precipitation respectively. Compared with observation data in 2002–2004, CFSR shows the best overall performance, followed by GLDAS, although the best ranking scores are different for different variables.
26	Lutz <i>et al.</i> (2014)	Gauge data (303 stations)	APHRODITE, CRU, ERA-Interim, PRINCETON	MB	1981–2010	APHRODITE is selected as the best data product to represent precipitation, and performance is very high during the monsoon months.
27	Zeng <i>et al.</i> (2012)	Gauge data	TRMM3B43v6	MB (Lancang River Basin)	1998–2009	TRMM3B43v6 demonstrates high accuracy in monitoring drought in Lancang River Basin

^a The full name of the acronyms and abbreviations in the table are listed at Appendix S1 in Supporting Information. Studies are reported in increasing from global scale to region scale then alphabetically within a year.

datasets (a) APHRODITE, (b) ERA-Interim, (c) PRINCETON, and (d) CRU using the quality controlled gauge data, finding that APHRODITE shows the best representation of precipitation, especially during the monsoon season. In comparison with gauge data, TRMM 3B43v6 has been evaluated for drought monitoring in the Lancang River Basin (Upper MB [UMB]) by Zeng *et al.* (2012), and a fair accuracy has been proved. Yet, a comprehensive investigation of the spatio-temporal variability of precipitation on the whole MB by using state-of-the-art, multi-source precipitation datasets (satellite and reanalysis precipitation data) is lacking.

As the spatio-temporal heterogeneous precipitation plays a key role in human living in the MB, a high spatio-temporal resolution gridded precipitation dataset could help deepen our understanding of precipitation changes and variability. Since the satellite and reanalysis precipitation data could offer an alternative solution with a fine spatio-temporal resolution to overcome the short-term and inhomogeneous gauge observations over the MB (Lutz *et al.*, 2014), the novelty of this study is to conduct a first assessment on the reliability of both satellite and reanalysis gridded precipitation datasets, with the ultimate goal to improve future precipitation assessments over the region.

This paper is structured as follows: the study area of the MB and data used are shown in section 2; the methodology applied is described in section 3; the results, including spatial and temporal variability, are presented in section 4; the overall reliability of the assessed products is discussed in section 5; and major concluding remarks are highlighted in section 6.

2 | STUDY AREA AND DATA

2.1 | Study area

The Mekong River is the 10th world's longest rivers at around 4,909 km, and the total land area of its basin is over 795,000 km² (Figure 1a) (MRC, 2010). Located in Southeast Asia, the Mekong River originates from the Tibetan Plateau in China, where the average mean elevation is over 4,000 m above sea level. It flows through Myanmar, Lao People's Democratic Republic (Lao PDR), Thailand, Cambodia, and Vietnam, before ending in the South China Sea. The river basin consists of two parts: that is, the Upper Basin in China and the Lower Basin in Mainland Southeast Asia. There are over 70 million people living in the MB with a population density around 88 inhabitants per km² (Pech and Sunada, 2008; FAO, 2011), and this number is expected to rapidly increase (Pech and Sunada, 2008). In the LMB, about 75% of the population live in rural areas and are closely linked to the river system although often lack access to basic government services and live below the poverty

line, especially in Lao PDR and Cambodia (MRC, 2010; FAO, 2011).

The annual average rainfall in the MB is around 1,370 mm, ranging from 1,257 to 1,557 mm for the 10-year (1998–2007) study period. The climate of the LMB is tropical monsoonal (MRC, 2010). June–October is the wet season, when the Indian Summer Monsoon (ISM) brings lot of moisture from the Indian Ocean and contributes to the annual precipitation of about 70% (i.e., ~995 mm). November–May is the dry season, with an average precipitation of 420 mm, when the East Asian Monsoon (EAM) with high-pressure systems occupies the MB (MRC, 2010; Delgado *et al.*, 2012). Supported by the ISM, a high amount of precipitation in the LMB in wet season is the major freshwater source of the Mekong River and extremely important for supplying agriculture water (Hoang *et al.*, 2016). During the dry season, less precipitation occurs, however, the snow-melt water from upstream contributes to the downstream Mekong River. Besides the ISM and EAM, the MB's climate is also affected by Tropical Cyclones (TCs) (MRC, 2010), as well as the El Niño–Southern Oscillation (ENSO) (Räsänen and Kummu, 2013). TC can induce a large amount of instantaneous precipitation in the MB by extreme rainfall events that may cause flooding. Meanwhile, the ENSO is associated with the interannual hydrometeorology and discharge variability (Räsänen and Kummu, 2013; Räsänen *et al.*, 2013), which could also lead to extreme water-related events. Due to the climate change, the non-stationary atmospheric circulations could be a reason for increasing hydroclimate change in the MB (Delgado *et al.*, 2010).

2.2 | Precipitation datasets

2.2.1 | Rain gauge-based observations

The Asian Precipitation—Highly Resolved Observational Data Integration Towards Evaluation (APHRODITE) is produced by the Research Institute for Humanity and Nature and the Meteorological Research Institute of Japan Meteorological Agency (<http://www.chikyuu.ac.jp/precip/english/index.html>; last accessed January 24, 2018) (Yatagai *et al.*, 2009; 2012). It is the only long-term and continental-scale daily product that was created primary with a dense network of daily rain gauge data for Asia (Tanarhte *et al.*, 2012). The data sources are: (a) the Global Telecommunications System-based data from the Global Surface Summary of the Day (<https://data.nodc.noaa.gov/cgi-bin/iso?id=gov.noaa.ncdc:C00516>; last accessed January 24, 2018); (b) data pre-compiled by other projects and organizations such as the daily rainfall data assembled by the Global Energy and Water Exchanges project Asian Monsoon Experiment—Tropics (GAME-T, <http://hydro.iis.u-tokyo.ac.jp/GAME-T/GAIN-T/index.html>; last accessed January 24, 2018), with a lot of routine (operational) observation datasets from all over the Southeast Asia collected in the framework of the GAME-T project; and (c) their own collection (Yatagai

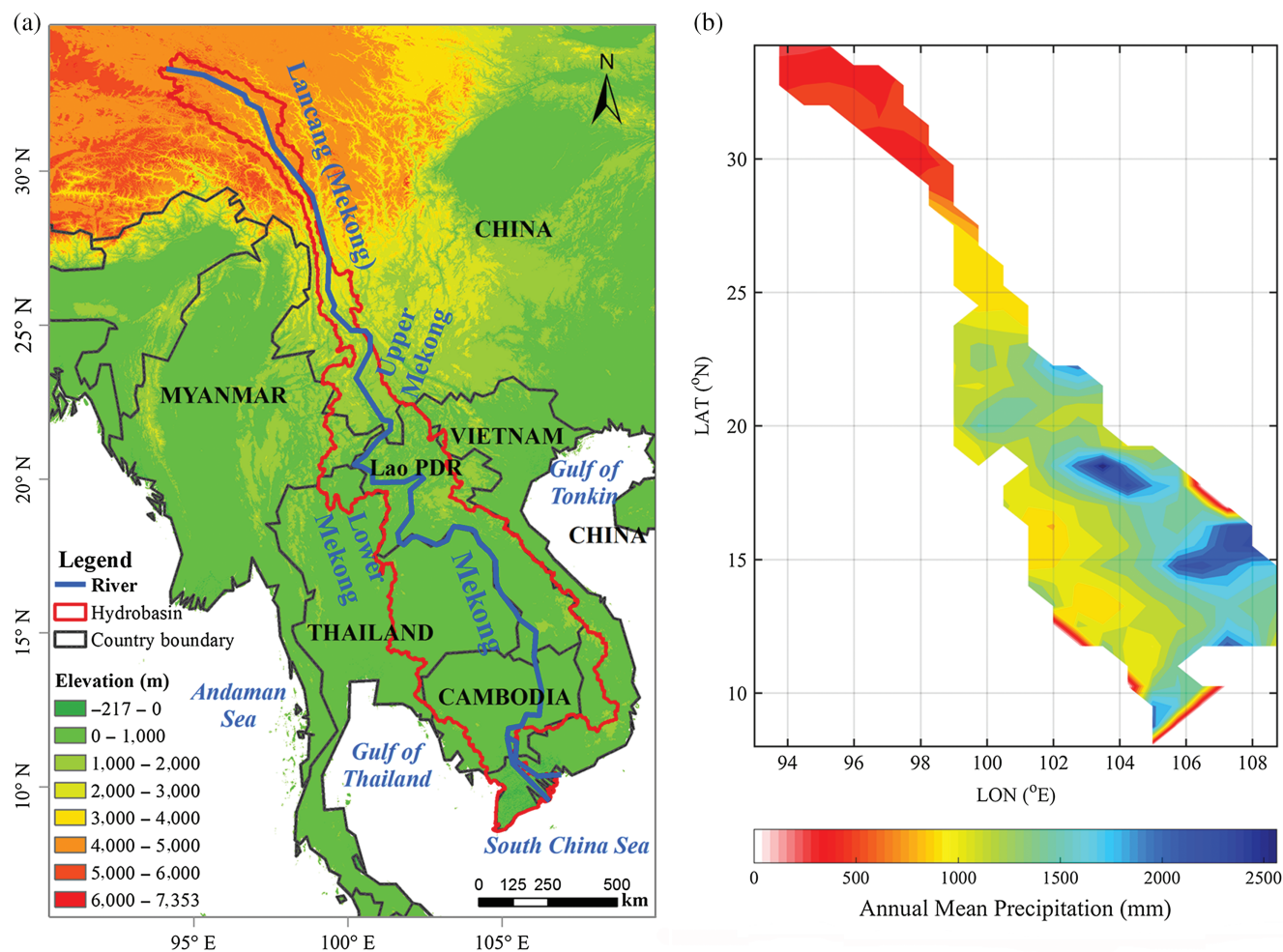


FIGURE 1 (a) Terrain map shows Southeast Asia and the MB. (b) Annual mean precipitation across the MB for 1998–2007

et al., 2012). More details on the data sources of APHRODITE can be found on the website (<http://www.chikyu.ac.jp/precip/>; last accessed January 24, 2018) and Yatagai *et al.* (2009). Though APHRODITE does not discriminate between rain and snow, it incorporates an improved quality-control method and orographic correction of precipitation (Yatagai *et al.*, 2012; Rana *et al.*, 2015). Moreover, APHRODITE has been chosen as a “ground truth” to evaluate multi-precipitation datasets derived from satellite and reanalysis products in many regions over monsoon-affected Asia such as Malaysia (Tan *et al.*, 2017), Central Asia (Sidike *et al.*, 2016), and East Asia (Sohn *et al.*, 2012). Furthermore, it was found that APHRODITE is useful for discharge modelling in the Mekong main stream (Lauri *et al.*, 2014). Though APHRODITE is of high quality gridded precipitation data, it should be kept in mind that APHRODITE has been turned out somewhat less precipitation compared to the Global Precipitation Climatology Centre (GPCC) data in the Mekong region (Yatagai *et al.*, 2012; Lauri *et al.*, 2014). Concerning both the overall performance of APHRODITE and the limited observations in the MB, the APHRODITE

was chosen as a reference dataset (hereafter reference data) for assessing the reliability of the other precipitation products, both from reanalysis and satellite (hereafter investigated data).

Reanalysis and satellite precipitation datasets to be evaluated against the APHRODITE reference product were selected using the following four criteria: (a) the spatial coverage must include the whole MB; (b) the spatial resolution must be higher than 1° ; (c) the temporal resolution should be at least at the daily scale; and (d) data have to be accessible in free and published databases. The selected precipitation datasets that meet the criteria include the CFSR, ERA-Interim, and the MERRA, Version 2 (MERRA2), as well as two satellite products, the Precipitation Estimation from Remote Sensing Information using an Artificial Neural Network—Climate Data Record (PERSIANN-CDR) and the TRMM post-real-time research products, version 7, 3B42v7 (TRMM 3B42). Details of each dataset are listed in Table 2 and domains of each dataset are shown in Figure S1, Supporting Information. These are described in the following subsections.

TABLE 2 Global precipitation datasets used in the MB

Type	Product	Temporal coverage	Spatial coverage	Spatial resolution	Temporal resolution	Reference
Gauge interpolation	APHRODITE	1951–2007	Eurasia 15°S–55°N, 60°E–150°E	0.25 × 0.25°	Daily	Yatagai <i>et al.</i> (2012)
Reanalysis	CFSR	1979–2011	Global	0.5 × 0.5°	6 hr	Saha <i>et al.</i> (2010)
	ERA-Interim	1979–present	Global	0.75 × 0.75°	6 hr	Dee <i>et al.</i> (2011)
	MERRA2	1980–present	Global	0.5 × 0.625°	1 hr	Gelaro <i>et al.</i> (2017)
Satellite	PERSIANN-CDR	1983–2015	60°N–60°S	0.25 × 0.25°	Daily	Ashouri <i>et al.</i> (2015)
	TRMM 3B42	1998–present	50°N–50°S	0.25 × 0.25°	3 hr	Huffman <i>et al.</i> (2007)

2.2.2 | Reanalysis data

By assimilating various observation inputs, reanalysis data provide an opportunity for numerous climate processes to be studied; however, the inhomogeneity and biases in observations and models can introduce spurious variability into reanalysis output (Lutz *et al.*, 2014). In our study, three reanalysis datasets are employed. First, the CFSR is a new coupled global reanalysis (third generation) from the National Centers for Environmental Prediction (NCEP, <https://rda.ucar.edu/pub/cfsr.html>; last accessed January 24, 2018) that is considerably more accurate than its predecessors because many known errors in the observational data ingested and the execution of previous reanalysis have been corrected (Saha *et al.*, 2010). However, relatively few evaluations of CFSR have been conducted, thus its performance is not well known (Saha *et al.*, 2010; Lutz *et al.*, 2014). Second, the ERA-Interim (<https://www.ecmwf.int/>; last accessed January 24, 2018) is a successive generation of ERA-40 produced by the ECMWF. It uses a 4D-variation data assimilation approach for the atmospheric analysis, with an improved representation of the hydrological cycle, a more realistic stratospheric circulation, and better temporal consistency on a range of timescales (Dee *et al.*, 2011). Finally, the MERRA2 (<https://gmao.gsfc.nasa.gov/reanalysis/MERRA-2/>; last accessed January 24, 2018) is produced by the NASA Global Modelling and Assimilation Office using the GEOS-5.12.4 system (Bosilovich *et al.*, 2015; Gelaro *et al.*, 2017). It replaces and extends the original MERRA reanalysis, and corrects the precipitation within the coupled atmosphere–land modelling system (Reichle *et al.*, 2017a). It also includes aerosol data assimilation and improved representations of aspects of the cryosphere and stratosphere, for example, ozone (Gelaro *et al.*, 2017). Nevertheless, further improvements in land surface hydrology estimates from reanalysis systems, including improvements in the approach used to impose precipitation corrections is needed for MERRA2 (Reichle *et al.*, 2017a).

2.2.3 | Satellite data

In comparison to the ground-based observations, satellite data provide precipitation data with a more complete converge (Nasrollahi *et al.*, 2013; Ashouri *et al.*, 2015). Besides, satellite precipitation data are being continuously improved,

and increasing amounts of satellite data are becoming available (Lutz *et al.*, 2014). Therefore, this provides a new opportunity for better and deeper research on global rainfall patterns. First, the PERSIANN-CDR (<http://chrsdata.eng.uci.edu/>; last accessed January 24, 2018), developed by the University of California in Irvine, estimates precipitation by an artificial neural network model which combines infrared (IR) and passive microwave measurement (PMW) information from multiple geostationary Earth orbiting (GEO) and low Earth orbit satellites. Further, the Global Precipitation Climatology Project (GPCP) monthly precipitation data are incorporated to bias adjustment (Sorooshian *et al.*, 2000; Ashouri *et al.*, 2015; Huang *et al.*, 2016a). As a high-resolution satellite dataset, PERSIANN-CDR is the only one to provide a time series of precipitation with sufficient length, consistency, and continuity to study the global and regional precipitation patterns and water cycle (Ashouri *et al.*, 2015; Liu *et al.*, 2017). Second, the TRMM 3B42 (<https://trmm.gsfc.nasa.gov/>; last accessed January 24, 2018) has been updated from version 6, combining PMW observations and IR data from GEO satellites to estimate precipitation, and the bias adjustments have been applied by using the GPCP monthly data (Huffman *et al.*, 2007; Huang *et al.*, 2016a; Huffman and Bolvin, 2017). Compared to version 6, the new TRMM 3B42 has advanced with additional satellite input, a new IR brightness temperature dataset, and uniformly reprocessed input data using current algorithms (Chen *et al.*, 2013).

3 | METHODOLOGY

In this study, an overlap period for all products was selected from January 1, 1998 to December 31, 2007 (i.e., 3,652 days). Owing to the distinct monsoon (June–October, wet season) and non-monsoon (November–May, dry season) seasons in the MB, the following evaluation is examined for these two seasons. First, we regrid data into a common 0.75 × 0.75° spatial resolution to match the lowest resolution dataset for a direct comparison. Three methods of regridding have been investigated: bilinear, bicubic, and distance-weighted average remapping by Climate Data Operators (<https://code.mpimet.mpg.de/projects/cdo/>; last accessed January 24, 2018). To identify eventual differences

among the three regriding methods, we calculated the correlation coefficient between each pair of the regrided fields by the three methods, at all the grids at monthly and annual scale, respectively. Results show that all the correlation coefficients are practically 1.0, indicating that there is almost no difference in the regrided fields by the three methods. Therefore, we used the results based on bilinear regriding.

Generally, the analysis is divided into two parts: (a) spatial averaged temporal variability on both annual and seasonal scales and (b) spatial variability. All the analyses on annual and seasonal timescales are conducted on the spatial mean, while the results on spatial variability are made at the gridded scale.

3.1 | Statistical methods

To evaluate the reliability of the investigated precipitation data, we employ four statistical measures including correlation coefficient (r), relative bias (RBS), normalized root-mean-square error (NRMSE), and Nash–Sutcliffe coefficient of efficiency (NS) (Nash and Sutcliffe, 1970; Moriasi *et al.*, 2007). Compared to the APHRODITE reference data, r draws the similarity of spatial distribution of investigated data, with the higher r the better performance; RBS measures the systematic overestimation or underestimation of the investigated data, and the smaller RBS the better performance; NRMSE measures the mean difference between two datasets, with the smaller NRMSE the smaller difference; and NS quantitatively describes the accuracy of the investigated data, with the higher NS showing the more accurate estimation. These four statistics are calculated by the following equations (see Equations 1–4). The correlation coefficient is also applied to describe the zonal and meridional precipitation anomaly, and spatial similarity of investigated data with respect to APHRODITE, respectively. Chiefly, a positive and significant r suggests good performance which resembles a similar precipitation pattern of reference data over the years and vice versa. Moreover, the statistical significance of r is tested at the confidence level of 95% ($p < .05$).

$$r = \frac{\sum_{i=1}^n (x_{\text{ref},i} - x'_{\text{ref}})(x_{\text{inv},i} - x'_{\text{inv}})}{\sqrt{\sum_{i=1}^n (x_{\text{ref},i} - x'_{\text{ref}})^2 \sum_{i=1}^n (x_{\text{inv},i} - x'_{\text{inv}})^2}} \quad (1)$$

$$\text{RBS} = \frac{\sum_{i=1}^n x_{\text{inv},i} - \sum_{i=1}^n x_{\text{ref},i}}{\sum_{i=1}^n x_{\text{ref},i}} * 100 \quad (2)$$

$$\text{NRMSE} = \frac{\sqrt{\frac{\sum_{i=1}^n (x_{\text{ref},i} - x_{\text{inv},i})^2}{n}}}{x'_{\text{ref}}} * 100 \quad (3)$$

$$\text{NS} = 1 - \left[\frac{\sum_{i=1}^n (x_{\text{inv},i} - x_{\text{ref},i})^2}{\sum_{i=1}^n (x_{\text{ref},i} - x'_{\text{ref}})^2} \right] \quad (4)$$

In Equations 1–4, x_{ref} denotes the reference data of APHRODITE, x_{inv} denotes the data being assessed, n is the total amount of data pairs that are calculated in this study, and i is the i th value of the time series, which is listed along the time. x'_{ref} and x'_{inv} are the means of the reference and investigated data over the time series, respectively.

For the reason that the assessed performance of the investigated data relies heavily on the type and number of assessment criteria being used (Schaller *et al.*, 2011; Fu *et al.*, 2013), a score-based method—Rank Score (RS) (Equations 5 and 6) has been employed to assess the overall performance of investigated data. In order to integrate the assessment of statistics for each investigated data at each temporal scale, we first evaluate the relative RS of the data in each individual assessment criteria (r , RBS, NRMSE, and NS, respectively). It should be noted that the RS for RBS and NRMSE are calculated by Equation 5, while r and NS are computed by Equation 6. This is because the former two show better performance with higher values, whereas the latter two show better performance with lower values.

$$\text{RS}_{i,j} = \frac{x_{i,j} - x_{i,\min}}{x_{i,\max} - x_{i,\min}} \quad (5)$$

$$\text{RS}_{i,j} = \frac{x_{i,j} - x_{i,\max}}{x_{i,\min} - x_{i,\max}} \quad (6)$$

In Equations 5 and 6, i represents the i th data (listing by CFSR, ERA-Interim, MERRA2, PERSIANN-CDR, TRMM 3B42), and $x_{i,\min}$ and $x_{i,\max}$ represent the data of minimum and maximum values of each assessment criteria. Thereafter, the four relative RS of the assessment criteria for each data are summed up to derive total RS at each temporal scale (annual, wet season, and dry season). Afterwards, the total RS for all the data at three temporal scales are obtained. Therefore, the total RS value is between 0 and 4, and the lower values means higher performance.

Meanwhile, the Taylor diagram is applied to visualize the statistic performance (Taylor, 2001). Besides the SD and r , the centre root-mean-square errors (CRMSEs) were visualized in the Taylor diagram. CRMSE is similar to the NRMSE, but has easier visualization characteristics in Taylor diagram which is calculated in Equation 7. Additionally, to evaluate the daily mean precipitation pattern in the MB for each dataset, we also evaluate the probability density functions (PDFs) of each temporal series.

$$\text{CRMSE} = \sqrt{\frac{\sum_{i=1}^n ((x_{\text{ref},i} - x'_{\text{ref}}) - (x_{\text{inv},i} - x'_{\text{inv}}))^2}{n}} \quad (7)$$

3.2 | Wavelets analysis

Wavelets analysis is a popular method in analysing the temporal variation of spectral properties in both stationary and non-stationary time series (Torrence and Compo, 1998; Taleb and Druyan, 2003; Kang and Lin, 2007). A practical and easy-to-use guide of wavelet analysis can be found in Torrence and Compo (1998). Wavelets analysis has been used for numerous studies in Hydrology (Labat *et al.*, 2005; Kang and Lin, 2007; Sang, 2013); and Geophysics (Torrence and Compo, 1998; Whitcher *et al.*, 2000), providing informations regarding the time frequency of the data. For example, Partal (2012) applied wavelet analysis to detect the characteristics and multi-variability of the runoff regime and precipitation of the Aegean region (Turkey). Taleb and Druyan (2003) showed that the African wave disturbances account for only a proportion of the seasonal precipitation in West Africa by using wavelet analysis. Yano and Jakubiak (2016) used wavelets for spatial verification of the quantitative precipitation forecasts. In the light of previous studies, we apply the wavelets analysis (Torrence and Compo, 1998) to detect the precipitation variability in both scale and time location of all the investigated data at the daily scale. By comparison, the reliability of each dataset will be evaluated by the correlation coefficient method with regard to the scale averaged time series of APHRODITE.

3.3 | Spatial variability

The spatial variability of the investigated data is evaluated by focusing on the relative value of precipitation to the range of precipitation, instead of comparing the absolute value. It will be described as follows. For the performance on spatial variability and trends, the relative precipitation at the maximum and minimum precipitation in the regions is calculated; the long-term trend and magnitude (unit: percentage to their annual mean precipitation for the whole MB for 1998–2007) are conducted using the Sen slope estimator (Sen, 1968) and Mann–Kendall methods with a confidence level of 95% ($p < .05$) (Kendall, 1938). This has been widely used in meteorological time series data (Feng and Zhou, 2012; Wu *et al.*, 2016; Atta-ur-Rahman and Dawood, 2017).

4 | RESULTS

4.1 | Temporal variability

Overall, all assessed datasets resemble the APHRODITE precipitation climatology averaged across the whole MB for 1998–2007, at annual, seasonal, and monthly timescales as shown in Figure 2 and summarized in Table 3. However, large differences in the amount of precipitation with respect to the reference data are found. To summarize: (a) among the investigated data, both satellite products (PERSIANN-CDR, TRMM 3B42) overestimate

precipitation at all timescales, as shown by the large gaps in precipitation at the annual and wet season scales (Figure 2a,b), with insignificant negative trends in annual and dry season measures (Table 3), whereas both show similar relative precipitation contributions to annual means during wet and dry seasons in comparison to the APHRODITE (Figure 2c); (b) for the reanalysis datasets, ERA-Interim (-8.2 mm yr^{-1}) stands out in capturing the annual precipitation trend, with the lowest gap between the APHRODITE reference data (-4.8 mm yr^{-1}) (Figure 2a, Table 3); (c) interestingly, all the reanalysis datasets overestimate annual precipitation, while the MERRA2 is the only one which displays the closest precipitation amount to the APHRODITE reference data, but with a slight underestimation after 2002 and significant downwards trends for all timescales (Figure 2a, Table 3); (d) in contrast, the CFSR strongly overestimates the precipitation amount at annual, seasonal, and monthly scales, with significant trend declines for the annual and dry season (Figure 2a, Table 3); (e) seasonal difference exists in trends of precipitation, with stronger declines in the dry season than the wet season (Table 3); and (f) finally, compared to the two satellite data (PERSIANN-CDR, TRMM 3B42), both reanalysis data (ERA-Interim and CFSR) show overestimation which is twice as strong in dry season than the wet (Table 3).

From the scatter plot of spatial averaged precipitation between each investigated data and reference data in both wet (Figure 3a) and dry (Figure 3b) seasons for 1998–2007, it is noticeable that: (a) all investigated data (except MERRA2) overestimate precipitation and (b) correlations to the reference are higher (and statistically significant) in dry season than the wet. In fact, for the dry season, the two satellite products (TRMM 3B42 and PERSIANN-CDR), as well as ERA-Interim, have relatively higher r values than the other reanalysis datasets (CFSR and MERRA2). In contrast, for the wet season, only TRMM 3B42 is significantly correlated ($p < .05$) to APHRODITE, denoting the higher accuracy of TRMM 3B42 in estimating precipitation for both seasons.

In light of the PDF method, the daily mean precipitation in each investigated dataset is evaluated in Figure 4. Generally, light rainfall events occur with high frequency in the MB, especially at amounts $<10 \text{ mm}$. Among the evaluated data, MERRA2 possesses almost the same shape of the APHRODITE's PDF, followed by ERA-Interim, TRMM 3B42, CFSR, and PERSIANN-CDR, but with a slight overestimation and underestimation at weak ($<10 \text{ mm}$) and moderate to heavy ($>10 \text{ mm}$) rainfall events, respectively. ERA-Interim shows the second highest similarity compared to APHRODITE, but underestimates light rainfall events and overestimates heavy ones. Both TRMM 3B42 and CFSR largely underestimate weak rainfall events by around two times compared to the reference data, while they also

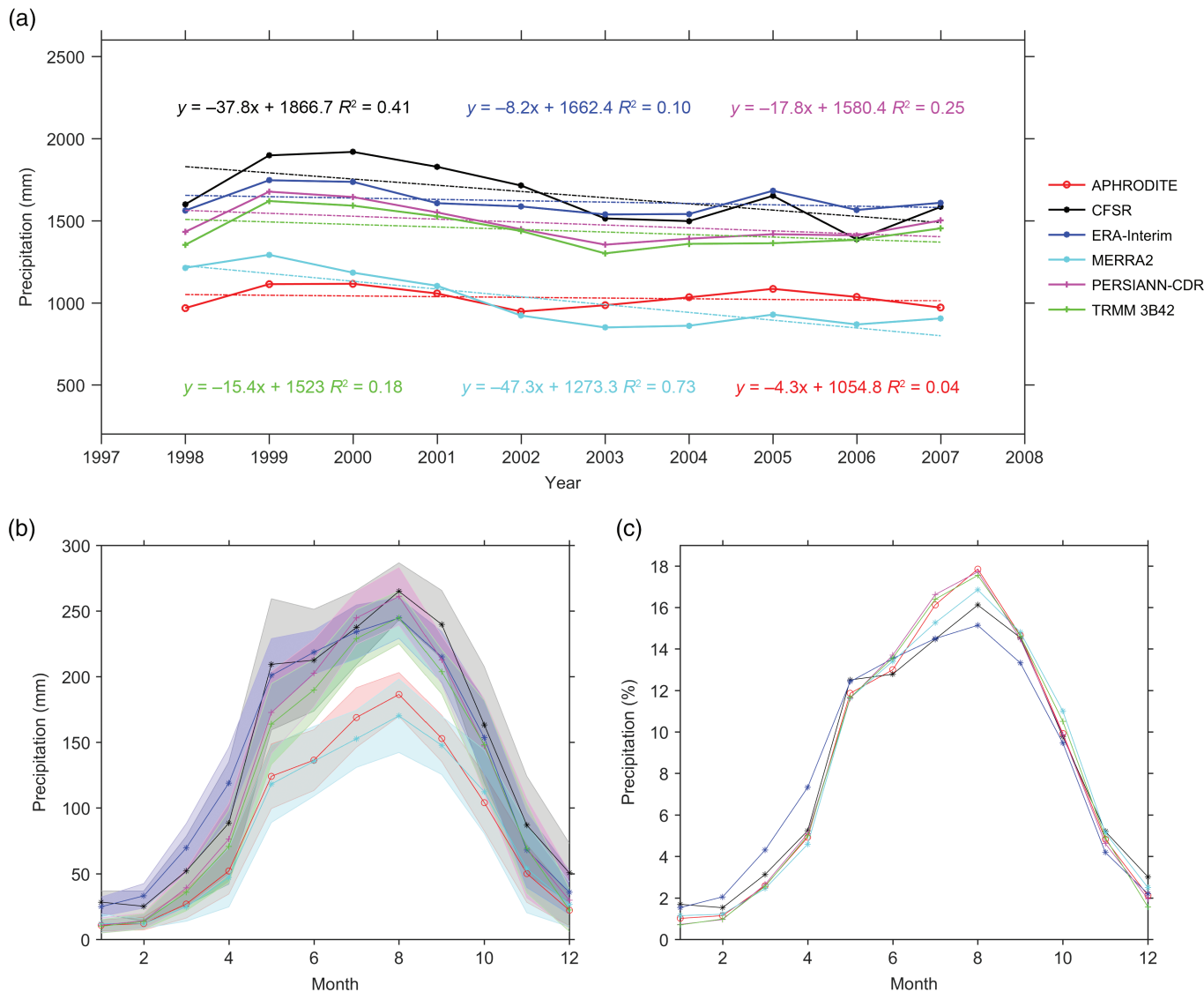


FIGURE 2 Precipitation for each investigated dataset in the MB for 1998–2007. (a) The annual mean precipitation over the MB along with the regression equations and coefficients of determination for each dataset. (b) The mean monthly precipitation over the MB. The shaded area represents the ± 1 unit SD. (c) The contribution of monthly precipitation (in %) to annual mean precipitation over the MB

overestimate the heavy rainfall events. Finally, PERSIANN-CDR presents the largest underestimation and overestimation at both weak and moderate to heavy rainfall events, respectively.

The statistical summary of precipitation shown in Table 3 highlights that both MERRA2 and TRMM 3B42 demonstrate better performance when compared to APHRODITE at all timescales for 1998–2007. Besides the closest mean values, MERRA2 shows the best performance with respect to the RBS, NRMSE, and NS. This is followed by the two satellite data, TRMM 3B42 and PERSIANN-CDR, which perform better than the other two reanalysis data regarding the mean, SD, RBS, NRMSE, and NS. Meanwhile, ERA-Interim behaves with a high reliability considering the trend and correlation coefficient. More interestingly, large differences in the correlation and bias performance between seasons were found. With respect to RBS and NRMSE, better performance in the dry season than the

wet exists in two satellite data, TRMM 3B42 and PERSIANN-CDR, whereas two reanalysis data (CFSR and ERA-Interim) display the opposite performance which is better in the wet season. In light of the total RS, the overall performance of the investigated data is led by MERRA2 and TRMM 3B42.

Visualizing the temporal statistic results of SD, CRMSE, and the correlation coefficient in the Taylor diagram (Figure 5) verifies the distinguish performance of each product. Generally, MERRA2 and TRMM 3B42 lead the reliability of gridded precipitation products regarding the statistical performance, characterized by relatively small SD and CRMSE, and relatively higher r values at all temporal scales (annual, wet season, dry season, and daily).

The spatial pattern of correlation coefficients between the investigated data and the APHRODITE reference at annual and both seasonal timescales is presented in Figure 6. Overall, there is a dominance of positive r values (over 76%)

TABLE 3 Summary of statistics on temporal data series

Statistics	Temporal	APHRODITE	CFSR	ERA-Interim	MERRA2	PERSIANN-CDR	TRMM 3B42
Mean (mm)	Annual	1,031.2	1,658.8	1,617.1	1,012.9	1,480.3	1,401.3
	Wet season	214.9	344.3	298.2	212.2	299.9	293.3
	Dry season	87.3	161.3	162.5	87.7	117.1	112.6
SD (mm)	Annual	147.2	274.1	206.9	224.8	200.7	189.0
	Wet season	34.9	54.6	38.4	42.6	38.1	37.7
	Dry season	22.0	51.5	36.4	32.9	35.3	33.2
Trend (mm y ⁻¹)	Annual	-4.8	-41.0*	-8.2	-47.0*	-15.6	-19.7
	Wet season	2.8	-13.8	3.9*	-23.8*	2.6	0.9
	Dry season	-13.8	-42.0*	-26.2	-31.9*	-30.3	-25.4
Relative difference of precipitation (%)	Annual	—	60.9	56.8	-1.8	43.8	39.5
	Wet season	—	49.3	42.3	-4.1	42.7	35.6
	Dry season	—	81.5	84.9	-1.2	38.2	29.4
<i>r</i>	Annual	—	0.5	0.8*	0.5	0.6	0.7*
	Wet season	—	0.1	0.6	0.1	0.6	0.7*
	Dry season	—	0.9*	1.0*	0.9*	0.9*	1.0*
RBS (%)	Annual	—	60.9	56.8	-1.8	43.5	35.9
	Wet season	—	60.2	38.7	-1.3	39.5	36.5
	Dry season	—	84.8	86.2	0.5	34.2	29.0
NRMSE (%)	Annual	—	62.5	57.0	13.9	44.3	36.5
	Wet season	—	61.7	39.2	13.5	40.2	37.0
	Dry season	—	91.4	86.9	17.4	38.1	31.7
NS	Annual	—	-119.7	-99.4	-4.9	-59.8	-40.3
	Wet season	—	-79.9	-31.6	-2.9	-33.2	-28.0
	Dry season	—	-27.1	-24.4	0.0	-3.9	-2.4
Total RS	Annual	—	3.7	2.6	1.0	2.4	1.7
	Wet season	—	4.0	1.7	1.0	1.8	1.4
	Dry season	—	4.0	2.8	0.7	1.0	0.6

*Statistically significant *r* were defined as those $p < .05$.

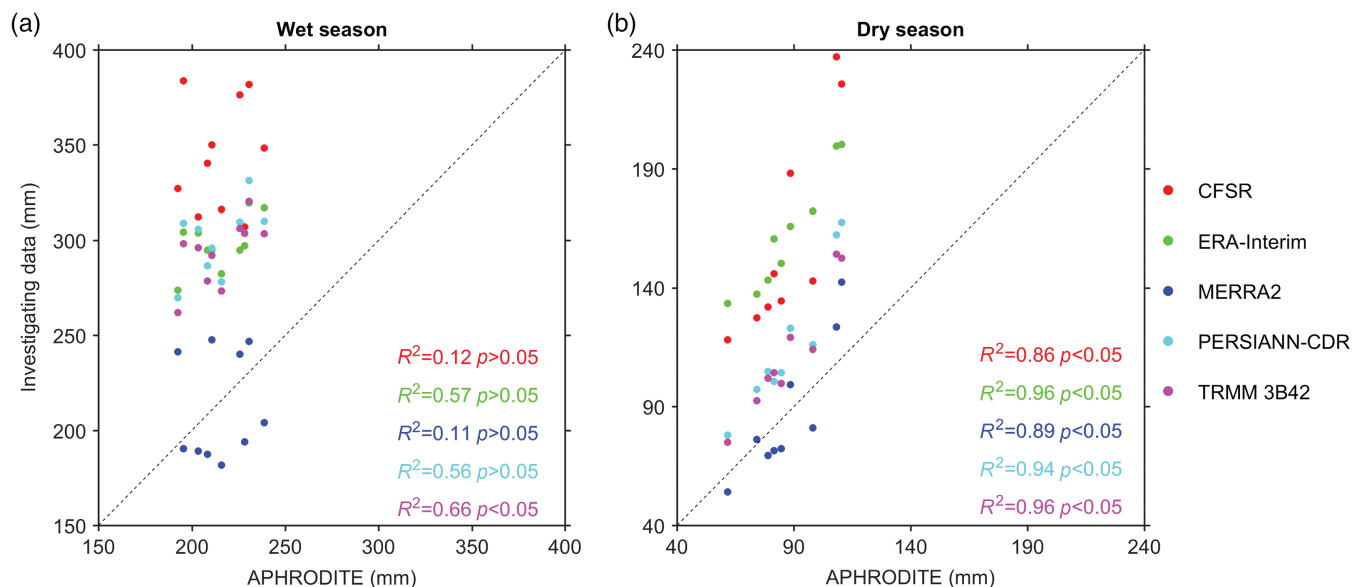


FIGURE 3 Comparison of precipitation between investigated data in (a) wet season and (b) dry season across the MB for 1998–2007

across the MB, indicating a general good performance of the investigated data. Negative *r*, however, exists in most of the investigated data over the southeast region at annual scale

(0.5–13%) and particularly the wet season (1–23.8%). Moreover, differences in the correlations with the APHRODITE reference are also found between seasons, with a larger

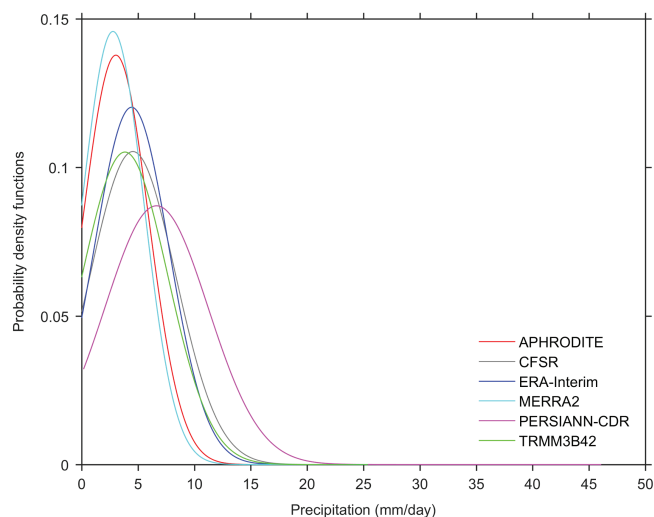


FIGURE 4 The PDFs of daily precipitation in the MB for 1998–2007

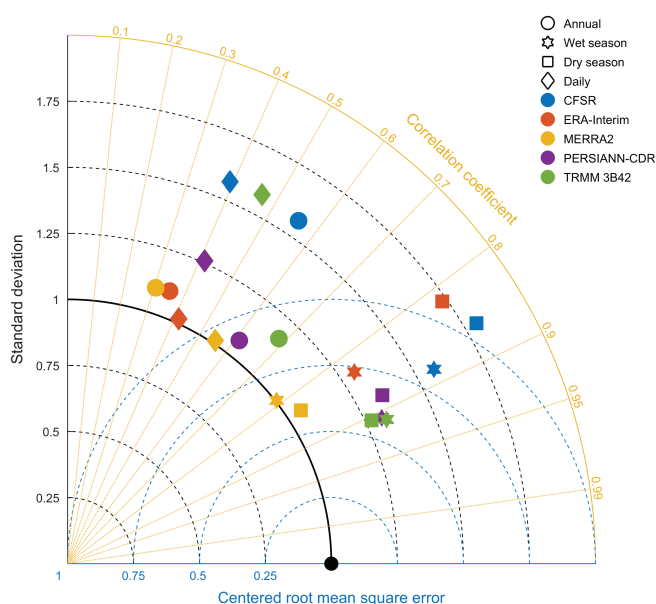


FIGURE 5 Taylor diagram of precipitation in the MB for 1998–2007, with shapes and colours indicating temporal scale and investigated data, respectively

extent of areas of higher (and statistically significant) r values in the dry season (47.7–80.8%) than the wet season (19.7–63.2%). In comparison to the other datasets, the TRMM 3B42 shows better performance when compared to the reference data by displaying positive and significant r values ($p < .05$) over the three temporal scales and across most of the region.

A wavelet power spectrum of APHRODITE daily precipitation across the MB for 1998–2007 is presented in Figure 7; and the investigated data present similar wavelet power spectrum (figures are not shown). Overall, an annual dominating scale of the precipitation variation is clearly captured. Besides, a number of small significant scales variabilities (<10 days) also exists. Power spectrums for the investigated data resemble similar features of the APHRODITE reference data. Moreover,

for comparing the averaged variance of small scales, the scale-average variance time series of all gridded data are displayed in Figure 8. With respect to APHRODITE, all of the evaluated data are significantly correlated to the reference data, with the highest r value in decreasing order by TRMM 3B42, MERRA2, ERA-Interim, CFSR, and PERSIANN-CDR.

Table 4 presents the correlation coefficient of zonal and meridional precipitation anomaly between APHRODITE and each investigated dataset at annual, wet and dry season scales for 1998–2007. Precipitation anomalies in all the data are significantly correlated to the reference data ($p < .05$) at the three temporal scales. Moreover, large seasonal differences were found with much higher r values in the dry season than in the wet. Among the investigated data, both satellite datasets (TRMM 3B42 and PERSIANN-CDR) highly and significantly correlate to APHRODITE, whereas the three reanalysis datasets (MERRA2, ERA-Interim, and CFSR) show roughly the same significant correlation to APHRODITE. Overall, all the assessed gridded data are able to capture the characteristics of precipitation variability across the MB, with the TRMM 3B42 showing better performance.

4.2 | Spatial variability

The patterns of spatial variability of mean precipitation in annual, wet, and dry seasons for 1998–2007 are shown in Figure 9. For the APHRODITE reference (Figure 9a1–a3), the precipitation increases from the northwest to the southeast of the region. In the LMB, there is a distinct west to east gradient with higher rainfall occurring in the east (Lao PDR) and lower rainfall occurring in the west (Thailand). During the wet season, a large area experiences high precipitation. Meanwhile, during the dry season such precipitation shrinks to a small area in the southeastern part of the region.

In terms of similarity, both TRMM 3B42 (Figure 9f1–f3) and CFSR (Figure 9b1–b3) show almost the same spatial distribution of precipitation when compared to APHRODITE at all timescales, denoting their ability to capture the spatial variability of precipitation across the MB. For other investigated datasets, PERSIANN-CDR (Figure 9e1–e3) resembles the high precipitation area over the centre of the region, but shows a larger area of high precipitation in the southeastern part when compared to the reference data; MERRA2 (Figure 9d1–d3) somehow underestimates precipitation in most of the region, with high precipitation centres in the southwest and southeast; and finally ERA-Interim (Figure 9c1–c3) has an abnormal precipitation centre in the west part of the middle MB.

Besides the spatial variability in mean precipitation, the distribution of trends in mean precipitation over the 10-year study period is also analysed in Figure 10. For the APHRODITE reference data, the precipitation trend is not statistically significant at the 95% confidence level over the basin

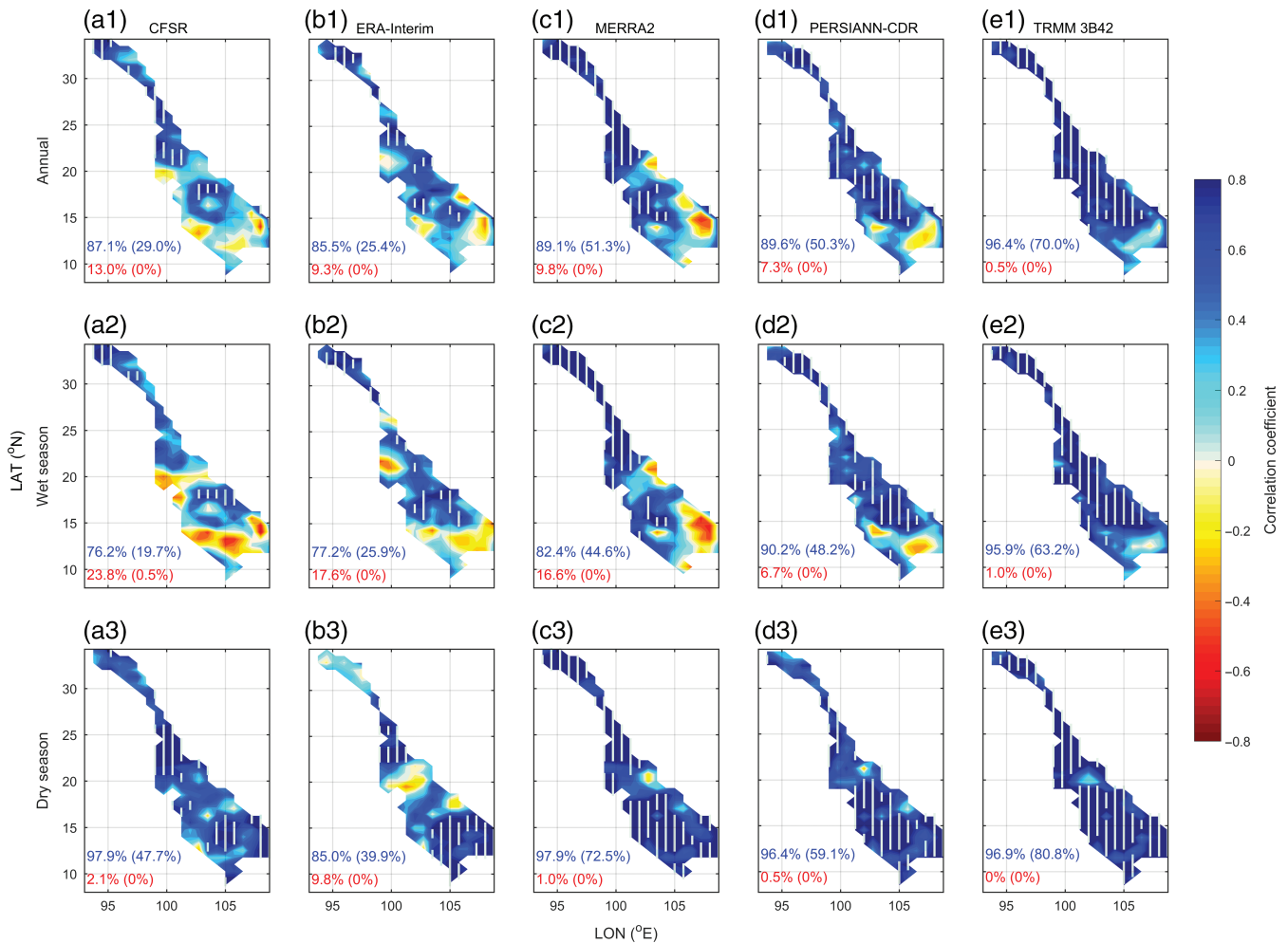


FIGURE 6 Spatial correlation coefficients of investigating precipitation data for CFSR (a1–a3), ERA-Interim (b1–b3), MERRA2 (c1–c3), PERSIANN-CDR (d1–d3), and TRMM 3B42 (e1–e3) with respect to APHRODITE at annual, wet, and dry season scales across the MB for 1998–2007. Trends with statistical significant correlations ($p < .05$) are marked in white vertical lines. Blue (red) numbers in each subfigure represent the percentage of area with positive (negative) r value, and the corresponding significant percentage is marked within the parentheses

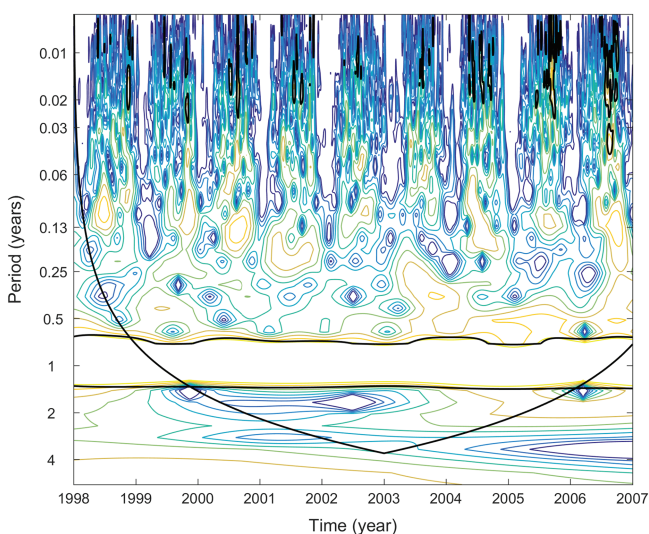


FIGURE 7 The wavelet power spectrum of APHRODITE daily precipitation

for all timescales; except for some negative trends in the northernmost part of the region. However, a distinct pattern

of trends in precipitation is found between the UMB (negative) and the LMB (positive) at both annual and wet season scales. For the dry season, a negative trend over most part of the basin is found which is of high magnitude but not significant in the southern part.

For the investigated data, both satellite products exhibit a high similarity of precipitation trends compared to the APHRODITE reference data; listed by TRMM 3B42 (Figure 10f1–f3) and PERSIANN-CDR (Figure 10e1–e3). For the reanalysis datasets, CFSR (Figure 10b1–b3) and MERRA2 (Figure 10d1–d3) show an overestimation of the magnitude and statistical significance of negative precipitation trends, especially in the LMB. Specifically, CFSR has high negative trends in Myanmar and northern Thailand, while MERRA2 shows significant negative trends in northern Lao PDR, Cambodia, and Vietnam. Finally, ERA-Interim (Figure 10c1–c3) presents an inconsistent spatial pattern in comparison to APHRODITE, with negative and positive precipitation trends in most parts of LMB and middle of the basin respectively.

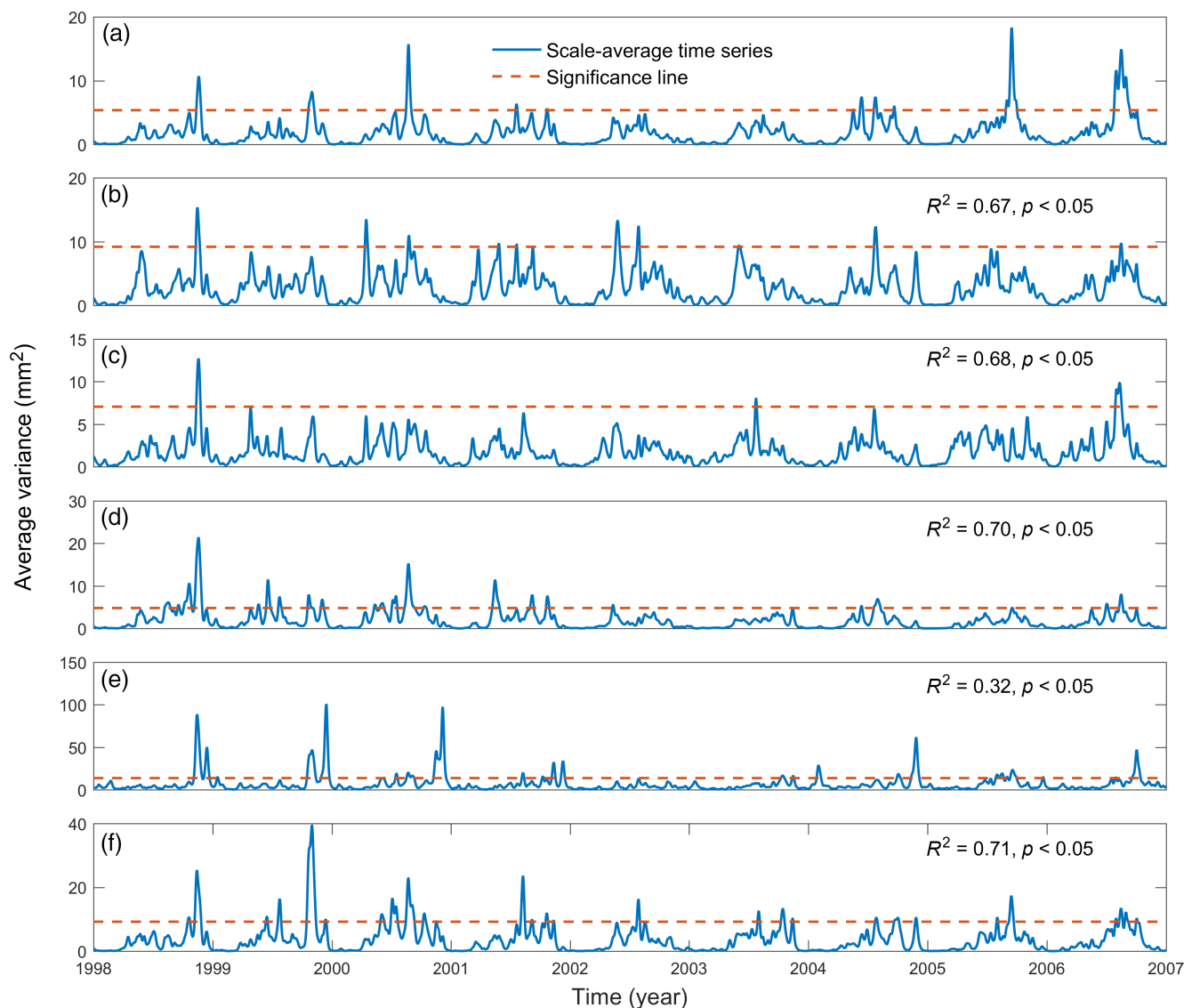


FIGURE 8 The scale average time series of daily precipitation wavelet analysis of gridded precipitation data: (a) APHRODITE, (b) CFSR, (c) ERA-Interim, (d) MERRA2, (e) PERSIANN-CDR, and (f) TRMM 3B42. The correlation coefficient between the scale average time series of each investigated dataset and APHRODITE is marked in the upper right panel, respectively [Colour figure can be viewed at wileyonlinelibrary.com]

TABLE 4 Correlation coefficients of zonal and meridional precipitation anomalies of investigated data with APHRODITE

Spatio-temporal scale	Zonal			Meridional		
	Annual	Wet season	Dry season	Annual	Wet season	Dry season
CFSR	0.47*	0.37*	0.74*	0.44*	0.29*	0.76*
ERA-Interim	0.48*	0.42	0.73	0.41	0.33	0.73
MERRA2	0.48	0.45	0.81	0.37	0.15	0.83
PERSIANN-CDR	0.57	0.57	0.79	0.55	0.56	0.86
TRMM 3B42	0.68	0.68	0.86	0.67	0.66	0.89

*Statistically significant r were defined as those $p < .05$.

5 | DISCUSSION

From the above assessment, most of the investigated datasets are able to capture the precipitation climatology of the MB for 1998–2007 when compared to the APHRODITE reference data. Among the investigated data, MERRA2 shows a good ability in estimating the absolute amount of

precipitation and its seasonal variability. It also performs well at resembling the precipitation distribution at the daily scale, with high similarity of PDF to APHRODITE. The precipitation corrections algorithm in MERRA2 (Gelaro *et al.*, 2017; Reichle *et al.*, 2017a; 2017b) could be the reason for its good performance. However, it is not reliable at seizing the spatial variability of precipitation in the MB because it

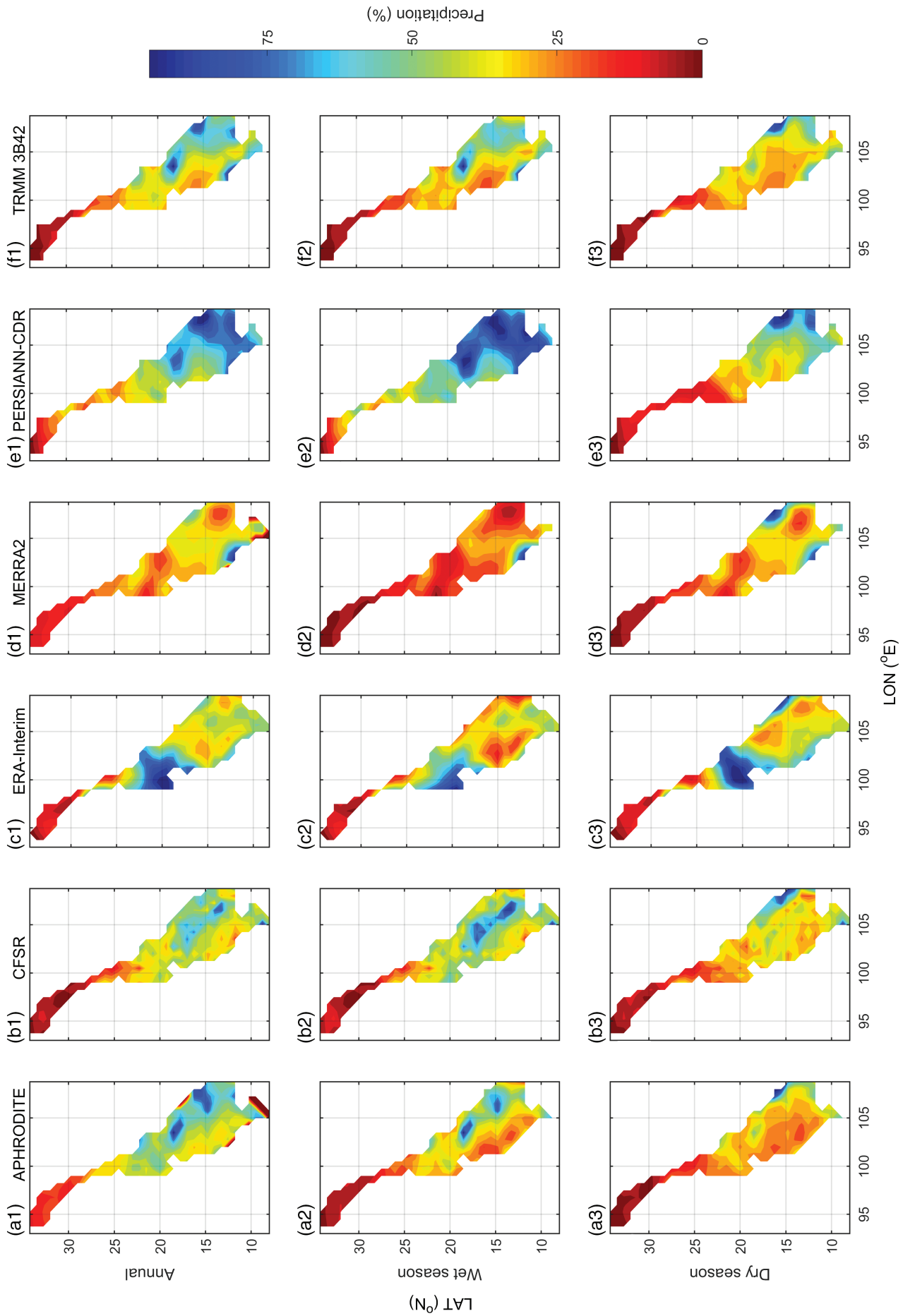


FIGURE 9 Spatial patterns of mean precipitation in the MB at annual, wet, and dry season scales for 1998–2007 with respect to their own range of precipitation. (a1–a3) APHRODITE, (b1–b3) CFSR, (c1–c3) ERA-Interim, (d1–d3) MERRA2, (e1–e3) PERSIANN-CDR, and (f1–f3) TRMM 3B42

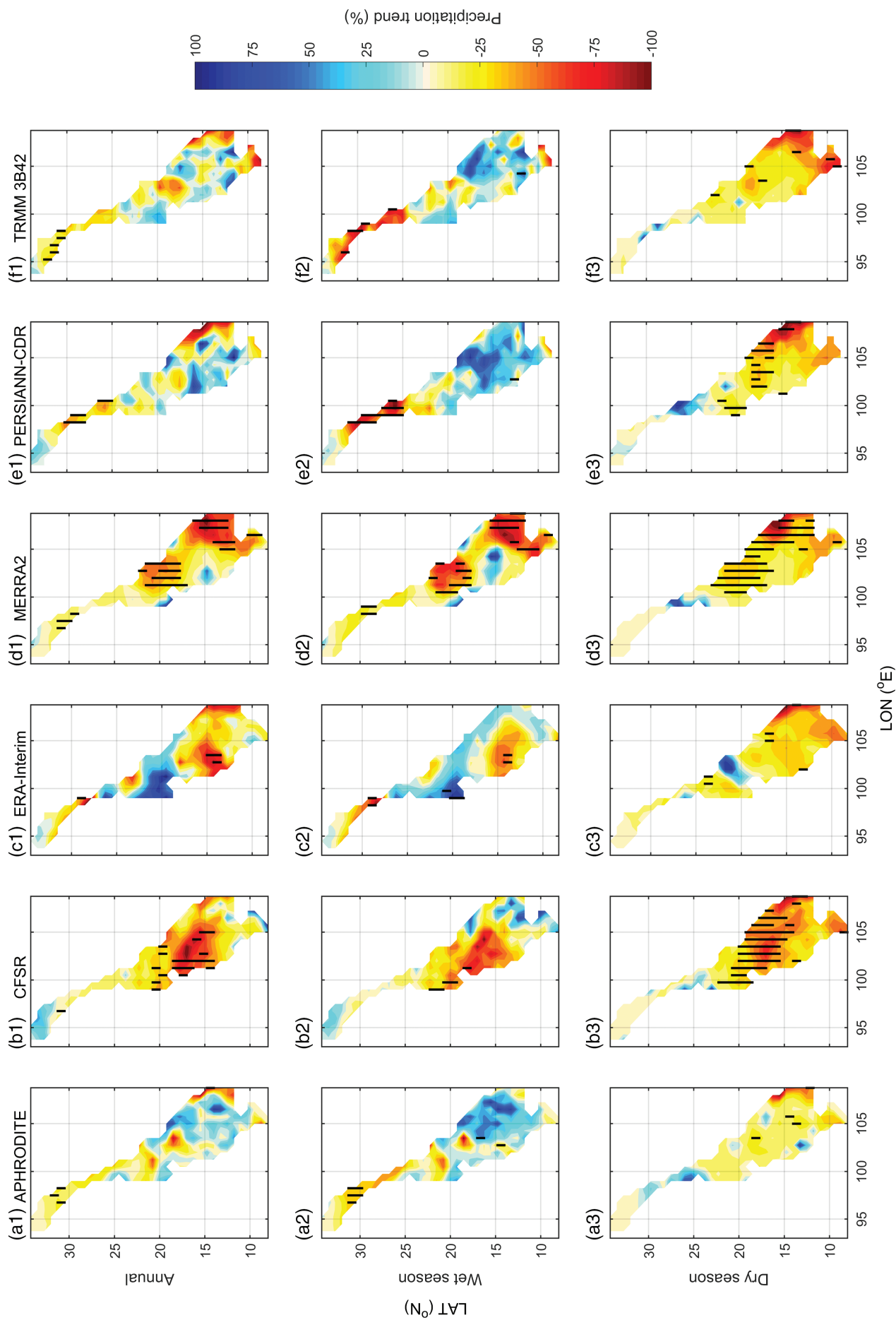


FIGURE 10 Spatial patterns of precipitation trends in the MB at annual, wet, and dry season scales for 1998–2007, at the 95% confidence level ($p < .05$). (a1–a3) APHRODITE, (b1–b3) CFSR, (c1–c3) ERA-Interim, (d1–d3) MERRA2, (e1–e3) PERSIANN-CDR, and (f1–f3) TRMM 3B42. Trends with significance are marked in black vertical lines

does not capture the precipitation centre in the study area, and also overestimates the significant negative precipitation trend in a large part of the region for 1998–2007. The reason behind this finding could be that MERRA2 does not include a land surface analysis, not counting precipitation corrections (Reichle *et al.*, 2017a).

CFSR does not show high reliability in assimilating the temporal variability of precipitation in the MB over the study period, and has the largest overestimations at annual and wet season periods. It also presents a rare significant negative trend of precipitation in most of LMB. According to Higgins *et al.* (2010) and Lorenz and Kunstmann (2012), an overactive diurnal cycle in the atmospheric component of CFSR may be a reason for the overestimation. Surprisingly, the spatial variabilities of mean precipitation at annual, wet, and dry season scales are well characterized by this reanalysis product. Though CFSR is a new coupled global reanalysis from NCEP, its performance is not well known because only a few evaluations have thus far been conducted (Saha *et al.*, 2010; Lutz *et al.*, 2014). Meanwhile, the ERA-Interim displays a relatively unreliable ability in estimating both the temporal and spatial variability, although it is good at resembling daily precipitation distribution and estimating the precipitation tendency over the study period. Both CFSR and ERA-Interim show a stronger overestimation in the dry season than PERSIANN-CDR and TRMM 3B42. The relatively poor performance of CFSR and ERA-Interim in this study coincides with Lauri *et al.* (2014) who comment that both cannot reproduce reliable spatial precipitation distribution, compared to APHRODITE and TRMM 3B42. Consequently, they do not provide accurate results for discharge modelling (Lorenz and Kunstmann, 2012; Lauri *et al.*, 2014). The unsatisfactory performance of reanalysis could be explained by the following: (a) the quality of reanalysis precipitation datasets relies heavily on the assimilated observation data, however, both the amount and spatial distribution of these observations change over time (Lorenz and Kunstmann, 2012) and (b) the observations for long-term climatological analysis in the MB remains questionable (Lutz *et al.*, 2014).

Compared to the reanalysis data, both satellite products, PERSIANN-CDR and TRMM 3B42, have the ability to estimate precipitation at both temporal and spatial scales which agrees with previous studies (Rana *et al.*, 2015; Tan *et al.*, 2017). TRMM 3B42 shows better performance compared to PERSIANN-CDR because it has more propinquity to APHRODITE on temporal variability (at annual and monthly scales), proven by the statistical results in Table 3. Furthermore, it is also better at capturing the spatial variability and trends of precipitation across the study area. Regarding the underestimation of precipitation in APHRODITE (Yatagai *et al.*, 2012; Lauri *et al.*, 2014), and the underestimation of MERRA2 compared to APHRODITE, TRMM 3B42 is more reliable at estimating the absolute amount of precipitation.

Because the LMB has suffered from increasing and long-lasting drought events (Delgado *et al.*, 2010), precipitation is extremely important for sustaining water supply in the MB. For instance, over the study period, a drought in 2003–2005 caused considerable agricultural losses in North East Thailand, Cambodia, and Lao PDR (Te, 2007; Räsänen *et al.*, 2013). As projected by Hoang *et al.* (2016), the increasing trend of droughts and floods over recent decades is going to continue in the future for part of the region. Drought events, however, are also about the timing of precipitation which means that particular atmospheric events could also induce extreme events (Te, 2007). Therefore, it is crucial that high resolution gridded precipitation datasets are able to grasp extreme precipitation features, which deserves to be deeply assessed in future research. However, the correlation coefficient of zonal and meridional precipitation anomaly between APHRODITE and each investigated dataset at annual, wet and dry season scales for 1998–2007 shown in Table 4, evaluates the performance of the investigated data in capturing the precipitation variability. Since they all significantly correlate to APHRODITE, it indicates that all the assessed datasets are able to estimate both of the zonal and meridional precipitation anomalies. Among them, TRMM 3B42 possesses the highest ability. As TRMM 3B42 has been widely used in TC rainfall studies (Chen *et al.*, 2013), it explains part of the high performance of TRMM 3B42. Meanwhile, TRMM 3B42 could yield equally good modelled discharge results by using ground observed precipitation data (Lauri *et al.*, 2014).

In view of our findings, the selection of precipitation datasets should be based on the aim of each study. APHRODITE could be a good choice for hydroclimate analysis; however, it is not available after 2007. PERSIANN-CDR has slightly less accuracy compared to TRMM 3B42, but offers an opportunity to study climatology over the globe by using satellite data since 1983 (Ashouri *et al.*, 2015). All three reanalysis datasets have long-term temporal coverage, which is crucial for hydro-climatological studies. Though TRMM started from 1998 and terminated in 2014, a new Global Precipitation Measurement project was launched to follow the highly successful TRMM (Huffman *et al.*, 2017). In addition, TRMM 3B42 has been proved to be able to estimate rainfall induced by TC (Chen *et al.*, 2013), which is a common event in the MB during the wet season (MRC, 2010). This also confirms the reliability of TRMM 3B42 in resembling precipitation in the MB.

6 | CONCLUSION

An evaluation on the reliability of both satellite and reanalysis precipitation datasets for the MB have been conducted in this study. The following major findings are drawn:

- (1) Most of the evaluated gridded datasets are able to capture the spatio-temporal variability of precipitation in the

MB for 1998–2007. Specifically, MERRA2 is reliable in terms of precipitation temporal variability with the lowest bias, but underestimates when compared to APHRODITE; TRMM 3B42 and PERSIANN-CDR show reliability in the variability of temporal series, while CFSR and ERA-Interim strongly overestimate the precipitation, especially in the dry season.

(2) Both satellite datasets (TRMM 3B42 and PERSIANN-CDR) present high reliabilities in capturing mean precipitation, as well as precipitation trends over the study period. Though CFSR overestimates precipitation on a temporal scale, it is able to describe the spatial pattern of precipitation, while both CFSR and MERRA2 present a large significant negative precipitation trend; and ERA-Interim has an inconsistent spatial variability when compared to APHRODITE.

(3) Overall, the TRMM 3B42 is the most reliable dataset in estimating precipitation in the MB, followed by the PERSIANN-CDR.

ACKNOWLEDGEMENTS

The authors wish to acknowledge Changgui Lin and Lorenzo Minola for their detailed and helpful comments and advice in the original manuscript, as well as C. Torrence and G. Compo who provided the wavelet analysis software at: URL: <http://paos.colorado.edu/research/wavelets/>. The authors also wish to acknowledge the anonymous reviewers for their detailed and helpful comments to the original manuscript. This research was supported by the Strategic Priority Research Program of Chinese Academy of Sciences (XDA20060401), the China Scholarship Council, the National Natural Science Foundation of China (91537210), Swedish STINT (CH2015-6226), and the European Union's Horizon 2020 research and innovation programme under the Marie Skłodowska-Curie grant agreement No. 703733.

ORCID

Deliang Chen  <http://orcid.org/0000-0003-0288-5618>

Cesar Azorin-Molina  <http://orcid.org/0000-0001-5913-7026>

REFERENCES

- Alijanian, M., Rakhshandehroo, G.R., Mishra, A.K. and Dehghani, M. (2017) Evaluation of satellite rainfall climatology using CMORPH, PERSIANN-CDR, PERSIANN, TRMM, MSWEP over Iran. *International Journal of Climatology*, 37(14), 4896–4914. <https://doi.org/10.1002/joc.5131>.
- Andersson, E., Bauer, P., Beljaars, A., Chevallier, F., Hólm, E., Janisková, M., Kallberg, P., Kelly, G., Lopez, P., McNally, A., Moreau, E., Simmons, A.J., Thépaut, J.N. and Tompkins, A.M. (2005) Assimilation and modeling of the atmospheric hydrological cycle in the ECMWF forecasting system. *Bulletin of the American Meteorological Society*, 86(3), 387–402. <https://doi.org/10.1175/BAMS-86-3-387>.
- Ashouri, H., Hsu, K.L., Sorooshian, S., Braithwaite, D.K., Knapp, K.R., Cecil, L.D., Nelson, B.R. and Prat, O.P. (2015) PERSIANN-CDR: daily precipitation climate data record from multisatellite observations for hydrological and climate studies. *Bulletin of the American Meteorological Society*, 96(1), 69–83. <https://doi.org/10.1175/BAMS-D-13-00068.1>.
- Atta-ur-Rahman and Dawood, M. (2017) Spatio-statistical analysis of temperature fluctuation using Mann–Kendall and Sen's slope approach. *Climate Dynamics*. Springer Berlin Heidelberg, 48(3–4), 783–797. <https://doi.org/10.1007/s00382-016-3110-y>.
- Bengtsson, L. (2010) The global atmospheric water cycle. *Environmental Research Letters*, 5(2), 025002. <https://doi.org/10.1088/1748-9326/5/2/025002>.
- Berg, W., L'Ecuyer, T. and Kummerow, C. (2006) Rainfall climate regimes: the relationship of regional TRMM rainfall biases to the environment. *Journal of Applied Meteorology and Climatology*, 45(3), 434–454. <https://doi.org/10.1175/JAM2331.1>.
- Bosilovich, M., Akella, S., Coy, L., Cullather, R., Draper, C., Gelaro, R., Kovach, R., Liu, Q., Molod, A., Norris, P., Wargan, K., Chao, W., Reichle, R., Takacs, L., Vikhliav, Y., Bloom, S., Collow, A., Firth, S., Labow, G., Partyka, G., Pawson, S., Reale, O., Schubert, S.D. and Suarez, M. (2015) MERRA-2 : initial evaluation of the climate. NASA Technical Report Series on Global Modeling and Data Assimilation, NASA/TM–2015-104606/Vol. 43, 139.
- Ceglar, A., Toreti, A., Balsamo, G. and Kobayashi, S. (2017) Precipitation over monsoon Asia: a comparison of reanalyses and observations. *Journal of Climate*, 30(2), 465–476. <https://doi.org/10.1175/JCLI-D-16-0227.1>.
- Chen, Y., Ebert, E.E., Walsh, K.J.E. and Davidson, N.E. (2013) Evaluation of TRMM 3B42 precipitation estimates of tropical cyclone rainfall using PACRAIN data. *Journal of Geophysical Research Atmospheres*, 118(5), 2184–2196. <https://doi.org/10.1002/jgrd.50250>.
- Decker, M., Brunke, M.A., Wang, Z., Sakaguchi, K., Zeng, X. and Bosilovich, M.G. (2012) Evaluation of the reanalysis products from GSFC, NCEP, and ECMWF using flux tower observations. *Journal of Climate*, 25(6), 1916–1944. <https://doi.org/10.1175/JCLI-D-11-00004.1>.
- Dee, D.P., Uppala, S.M., Simmons, A.J., Berrisford, P., Poli, P., Kobayashi, S., Andrae, U., Balmaseda, M.A., Balsamo, G., Bauer, P., Bechtold, P., Beljaars, A.C.M., van de Berg, L., Bidlot, J., Bormann, N., Delsol, C., Dragani, R., Fuentes, M., Geer, A.J., Haimberger, L., Healy, S.B., Hersbach, H., Hólm, E.V., Isaksen, I., Kållberg, P., Köhler, M., Matricardi, M., McNally, A.P., Monge-Sanz, B.M., Morcrette, J.J., Park, B.K., Peubey, C., de Rosnay, P., Tavolato, C., Thépaut, J.N. and Vitart, F. (2011) The ERA-interim reanalysis: configuration and performance of the data assimilation system. *Quarterly Journal of the Royal Meteorological Society*, 137(656), 553–597. <https://doi.org/10.1002/qj.828>.
- Delgado, J.M., Merz, B. and Apel, H. (2010) Flood trends and variability in the Mekong river. *Assembly*, 14, 407–418.
- Delgado, J.M., Merz, B. and Apel, H. (2012) A climate-flood link for the lower Mekong River. *Hydrology and Earth System Sciences*, 16(5), 1533–1541. <https://doi.org/10.5194/hess-16-1533-2012>.
- FAO. (2011) Mekong River Basin. Irrigation in Southern and Eastern Asia in Figures—AQUASTAT Survey—2011. Rome: Food and Agriculture Organization of the United Nations (FAO). pp. 1–16.
- Feng, L. and Zhou, T. (2012) Water vapor transport for summer precipitation over the Tibetan Plateau: multidata set analysis. *Journal of Geophysical Research Atmospheres*, 117(20), 1–16. <https://doi.org/10.1029/2011JD017012>.
- Fu, G., Liu, Z., Charles, S.P., Xu, Z. and Yao, Z. (2013) A score-based method for assessing the performance of GCMs: a case study of southeastern Australia. *Journal of Geophysical Research Atmospheres*, 118(10), 4154–4167. <https://doi.org/10.1002/jgrd.50269>.
- Gao, Y.C. and Liu, M.F. (2013) Evaluation of high-resolution satellite precipitation products using rain gauge observations over the Tibetan Plateau. *Hydrology and Earth System Sciences*, 17(2), 837–849. <https://doi.org/10.5194/hess-17-837-2013>.
- Gebregiorgis, A.S. and Hossain, F. (2015) How well can we estimate error variance of satellite precipitation data around the world? *Atmospheric Research*. Elsevier B.V., 154, 39–59. <https://doi.org/10.1016/j.atmosres.2014.11.005>.
- Gelaro, R., McCarty, W., Suárez, M.J., Todling, R., Molod, A., Takacs, L., Randles, C.A., Darmenov, A., Bosilovich, M.G., Reichle, R., Wargan, K., Coy, L., Cullather, R., Draper, C., Akella, S., Buchard, V., Conaty, A., da Silva, A.M., Gu, W., Kim, G.K., Koster, R., Lucchesi, R., Merkova, D., Nielsen, J.E., Partyka, G., Pawson, S., Putman, W., Rienecker, M., Schubert, S.D., Sienkiewicz, M. and Zhao, B. (2017) The modern-era retrospective analysis for research and applications, version 2 (MERRA-2).

- Journal of Climate*, 30(14), 5419–5454. <https://doi.org/10.1175/JCLI-D-16-0758.1>.
- Held, I.M. and Soden, B.J. (2000) Water vapor feedback and global warming. *Annual Review of Energy and the Environment*, 25(1), 441–475. <https://doi.org/10.1146/annurev.energy.25.1.441>.
- Higgins, R.W., Kousky, V.E., Silva, V.B.S., Becker, E. and Xie, P. (2010) Intercomparison of daily precipitation statistics over the United States in observations and in NCEP reanalysis products. *Journal of Climate*, 23(17), 4637–4650. <https://doi.org/10.1175/2010JCLI3638.1>.
- Hoang, L.P., Lauri, H., Kumm, M., Koponen, J., Vliet, M.T.H.V., Supit, I., Leemans, R., Kabat, P. and Ludwig, F. (2016) Mekong River flow and hydrological extremes under climate change. *Hydrology and Earth System Sciences*, 20(7), 3027–3041. <https://doi.org/10.5194/hess-20-3027-2016>.
- Huang, A., Zhao, Y., Zhou, Y., Yang, B., Zhang, L., Dong, X., Fang, D. and Wu, Y. (2016a) Evaluation of multisatellite precipitation products by use of ground-based data over China. *Journal of Geophysical Research: Atmospheres*, 121, 10654–10675. <https://doi.org/10.1002/2016JD025456>.
- Huang, D.Q., Zhu, J., Zhang, Y.C., Huang, Y. and Kuang, X.Y. (2016b) Assessment of summer monsoon precipitation derived from five reanalysis datasets over East Asia. *Quarterly Journal of the Royal Meteorological Society*, 142(694), 108–119. <https://doi.org/10.1002/qj.2634>.
- Huffman, G.J. and Bolvin, D.T. (2017) TRMM and other data precipitation data set documentation (ftp://meso-a.gsfc.nasa.gov/pub/trmmdocs/3B42_3B43_doc.pdf). Goddard Space Flight Center, NASA, (April), pp. 1–3.
- Huffman, G.J., Bolvin, D.T. and Nelkin, E.J. (2017) Integrated multi-satellite retrievals for GPM (IMERG) technical documentation. NASA, 3(2), e000469. <https://doi.org/10.1136/openhrt-2016-000469>.
- Huffman, G.J., Bolvin, D.T., Nelkin, E.J., Wolff, D.B., Adler, R.F., Gu, G., Hong, Y., Bowman, K.P. and Stocker, E.F. (2007) The TRMM multisatellite precipitation analysis (TMPA): quasi-global, multiyear, combined-sensor precipitation estimates at fine scales. *Journal of Hydrometeorology*, 8(1), 38–55. <https://doi.org/10.1175/JHM560.1>.
- IPCC. (2013) Climate change 2013: the physical science basis. In: Stocker, T.F., Qin, D., Plattner, G.-K., Tignor, M., Allen, S.K., Boschung, J., Nauels, A., Xia, Y., Bex, V. and Midgley, P.M. (Eds.) *Contribution of Working Group I to the Fifth Assessment Report of the Intergovernmental Panel on Climate Change*. Cambridge and New York, NY: Cambridge University Press, 1535 pp.
- Kang, S. and Lin, H. (2007) Wavelet analysis of hydrological and water quality signals in an agricultural watershed. *Journal of Hydrology*, 338, 1–14. <https://doi.org/10.1016/j.jhydrol.2007.01.047>.
- Kendall, M.G. (1938) A new measure of rank correlation. *Biometrika*, 30(1/2), 81. <https://doi.org/10.2307/2332226>.
- Kidd, C., Bauer, P., Turk, J., Huffman, G.J., Joyce, R., Hsu, K.-L. and Braithwaite, D. (2012) Intercomparison of high-resolution precipitation products over Northwest Europe. *Journal of Hydrometeorology*, 13(1), 67–83. <https://doi.org/10.1175/JHM-D-11-042.1>.
- Kirstetter, P.-E., Hong, Y., Gourley, J.J., Schwaller, M., Petersen, W. and Zhang, J. (2013) Comparison of TRMM 2A25 products, version 6 and version 7, with NOAA/NSSL ground radar-based National Mosaic QPE. *Journal of Hydrometeorology*, 14(2), 661–669. <https://doi.org/10.1175/JHM-D-12-030.1>.
- Koutsouris, A.J., Chen, D. and Lyon, S.W. (2016) Comparing global precipitation data sets in eastern Africa: a case study of Kilombero Valley, Tanzania. *International Journal of Climatology*, 36(4), 2000–2014. <https://doi.org/10.1002/joc.4476>.
- Labat, D., Ronchail, J. and Loup, J. (2005) Recent advances in wavelet analyses: part 2—amazon, Parana, Orinoco and Congo discharges time scale variability. *Journal of Hydrology*, 314, 289–311. <https://doi.org/10.1016/j.jhydrol.2005.04.004>.
- Lauri, H., Räsänen, T.A., Kumm, M., Lauri, H., Räsänen, T.A. and Kumm, M. (2014) Using reanalysis and remotely sensed temperature and precipitation data for hydrological modeling in monsoon climate: Mekong River case study. *Journal of Hydrometeorology*, 15(4), 1532–1545. <https://doi.org/10.1175/JHM-D-13-084.1>.
- Liu, X., Yang, T., Hsu, K., Liu, C. and Sorooshian, S. (2017) Evaluating the streamflow simulation capability of PERSIANN-CDR daily rainfall products in two river basins on the Tibetan plateau. *Hydrology and Earth System Sciences*, 21(1), 169–181. <https://doi.org/10.5194/hess-21-169-2017>.
- Lorenz, C. and Kunstmann, H. (2012) The hydrological cycle in three state-of-the-art Reanalyses: intercomparison and performance analysis. *Journal of Hydrometeorology*, 13(5), 1397–1420. <https://doi.org/10.1175/JHM-D-11-088.1>.
- Lutz, A., Terink, W., Droogers, P., Immerzeel, W. and Piman, T. (2014) *Development of baseline climate data set and trend analysis in the Mekong Basin*. Wageningen, The Netherlands, pp. 1–127.
- Moriasi, D.N., Arnold, J.G., Van Liew, M.W., Bingner, R.L., Harmel, R.D. and Veith, T.L. (2007) Model evaluation guidelines for systematic quantification of accuracy in watershed simulations. *Transactions of the ASABE*, 50(3), 885–900.
- MRC. (2010) State of the Basin Report 2010. Mekong River Commission. Vientiane, Lao PDR. 1728, 3248.
- Nash, J.E. and Sutcliffe, J.V. (1970) River flow forecasting through conceptual models part I—a discussion of principles*. *Journal of Hydrology*, 10, 282–290. [https://doi.org/10.1016/0022-1694\(70\)90255-6](https://doi.org/10.1016/0022-1694(70)90255-6).
- Nasrollahi, N., Hsu, K. and Sorooshian, S. (2013) An artificial neural network model to reduce false alarms in satellite precipitation products using MODIS and CloudSat observations. *Journal of Hydrometeorology*, 14(6), 1872–1883. <https://doi.org/10.1175/JHM-D-12-0172.1>.
- Partal, T. (2012) Wavelet analysis and multi-scale characteristics of the runoff and precipitation series of the Aegean region (Turkey). *International Journal of Climatology*, 32(1), 108–120. <https://doi.org/10.1002/joc.2245>.
- Pascale, S., Lucarini, V., Feng, X., Porporato, A. and Hasson, S. (2015) Analysis of rainfall seasonality from observations and climate models. *Climate Dynamics*. Springer Berlin Heidelberg, 44(11–12), 3281–3301. <https://doi.org/10.1007/s00382-014-2278-2>.
- Pech, S. and Sunada, K. (2008) Population growth and natural-resources pressures in the Mekong River Basin. *AMBIO*, 37(1), 219–224. [https://doi.org/10.1579/0044-7447\(2008\)37\[219:PGANPI\]2.0.CO;2](https://doi.org/10.1579/0044-7447(2008)37[219:PGANPI]2.0.CO;2).
- Piessens, M. (2016) *Livelihoods and Food Security on the Mekong River*. Dalkeith: Future Directions International, pp. 1–7.
- Ramanathan, V. (2001) Aerosols, climate, and the hydrological cycle. *Science*, 294(5549), 2119–2124. <https://doi.org/10.1126/science.1064034>.
- Rana, S., McGregor, J. and Renwick, J. (2015) Precipitation seasonality over the Indian subcontinent: an evaluation of gauge, reanalyses, and satellite retrievals. *Journal of Hydrometeorology*, 16(2), 631–651. <https://doi.org/10.1175/JHM-D-14-0106.1>.
- Räsänen, T.A. and Kumm, M. (2013) Spatiotemporal influences of ENSO on precipitation and flood pulse in the Mekong River Basin. *Journal of Hydrology*, 476, 154–168. <https://doi.org/10.1016/j.jhydrol.2012.10.028>.
- Räsänen, T.A., Lehr, C., Mellin, I., Ward, P.J. and Kumm, M. (2013) Palaeoclimatological perspective on river basin hydrometeorology: case of the Mekong Basin. *Hydrology and Earth System Sciences*, 17(5), 2069–2081. <https://doi.org/10.5194/hess-17-2069-2013>.
- Reichle, R.H., Draper, C.S., Liu, Q., Girotto, M., Mahanama, S.P.P., Koster, R. D. and De Lannoy, G.J.M. (2017a) Assessment of MERRA-2 land surface hydrology estimates. *Journal of Climate*, 30(8), 2937–2960. <https://doi.org/10.1175/JCLI-D-16-0720.1>.
- Reichle, R.H., Liu, Q., Koster, R.D., Draper, C.S., Mahanama, S.P.P. and Partyka, G.S. (2017b) Land surface precipitation in MERRA-2. *Journal of Climate*, 30(5), 1643–1664. <https://doi.org/10.1175/JCLI-D-16-0570.1>.
- Saha, S., Moorthi, S., Pan, H.L., Wu, X., Wang, J., Nadiga, S., Tripp, P., Kistler, R., Woollen, J., Behringer, D., Liu, H., Stokes, D., Grumbine, R., Gayno, G., Wang, J., Hou, Y.T., Chuang, H.Y., Juang, H.M.H., Sela, J., Iredell, M., Treadon, R., Kleist, D., Van Delst, P., Keyser, D., Derber, J., Ek, M., Meng, J., Wei, H., Yang, R., Lord, S., Van Den Dool, H., Kumar, A., Wang, W., Long, C., Chelliah, M., Xue, Y., Huang, B., Schemm, J.K., Ebisuzaki, W., Lin, R., Xie, P., Chen, M., Zhou, S., Higgins, W., Zou, C.Z., Liu, Q., Chen, Y., Han, Y., Cucurull, L., Reynolds, R.W., Rutledge, G. and Goldberg, M. (2010) The NCEP climate forecast system reanalysis. *Bulletin of the American Meteorological Society*, 91(8), 1015–1057. <https://doi.org/10.1175/2010BAMS3001.1>.
- Salio, P., Hobouchian, M.P., García Skabar, Y. and Vila, D. (2015) Evaluation of high-resolution satellite precipitation estimates over southern South America using a dense rain gauge network. *Atmospheric Research*. Elsevier B.V., 163, 146–161. <https://doi.org/10.1016/j.atmosres.2014.11.017>.
- Sang, Y. (2013) A review on the applications of wavelet transform in hydrology time series analysis. *Atmospheric Research*. Elsevier B.V., 122, 8–15. <https://doi.org/10.1016/j.atmosres.2012.11.003>.
- Schaller, N., Mahlstein, I., Cermak, J. and Knutti, R. (2011) Analyzing precipitation projections: a comparison of different approaches to climate model

- evaluation. *Journal of Geophysical Research Atmospheres*, 116(10), 1–14. <https://doi.org/10.1029/2010JD014963>.
- Sen, P.K. (1968) Estimates of the regression coefficient based on Kendall's tau. *Journal of the American Statistical Association*, 63(324), 1379–1389. <https://doi.org/10.1080/01621459.1968.10480934>.
- Seyyedi, H., Anagnostou, E.N., Beighley, E. and McCollum, J. (2015) Hydrologic evaluation of satellite and reanalysis precipitation datasets over a mid-latitude basin. *Atmospheric Research*. Elsevier B.V., 164–165, 37–48. <https://doi.org/10.1016/j.atmosres.2015.03.019>.
- Sidike, A., Chen, X., Liu, T., Durdiev, K. and Huang, Y. (2016) Investigating alternative climate data sources for hydrological simulations in the upstream of the Amu Darya river. *Water (Switzerland)*, 8(10), 441. <https://doi.org/10.3390/w8100441>.
- Sohn, S.J., Tam, C.Y., Ashok, K. and Ahn, J.B. (2012) Quantifying the reliability of precipitation datasets for monitoring large-scale East Asian precipitation variations. *International Journal of Climatology*, 32(10), 1520–1526. <https://doi.org/10.1002/joc.2380>.
- Sorooshian, S., Hsu, K.L., Gao, X., Gupta, H.V., Imam, B. and Braithwaite, D. (2000) Evaluation of PERSIANN system satellite-based estimates of tropical rainfall. *Bulletin of the American Meteorological Society*, 81(9), 2035–2046. [https://doi.org/10.1175/1520-0477\(2000\)081<2035:EOPSSE>2.3.CO;2](https://doi.org/10.1175/1520-0477(2000)081<2035:EOPSSE>2.3.CO;2).
- Su, F. and Hao, Z. (2001) Review of land-surface hydrological processes parameterization. *Advance in Earth Sciences*, 16(6), 795–801 (In Chinese).
- Taleb, E.H. and Druyan, L.M. (2003) Relationships between rainfall and West African wave disturbances in station observations. *International Journal of Climatology*, 23(3), 305–313. <https://doi.org/10.1002/joc.883>.
- Tan, M.L., Gassman, P.W. and Cracknell, A.P. (2017) Assessment of three long-term gridded climate products for hydro-climatic simulations in tropical river basins. *Water (Switzerland)*, 9(3), 229. <https://doi.org/10.3390/w9030229>.
- Tanarhte, M., Hadjinicolaou, P. and Lelieveld, J. (2012) Intercomparison of temperature and precipitation data sets based on observations in the Mediterranean and the Middle East. *Journal of Geophysical Research Atmospheres*, 117(12), D12102. <https://doi.org/10.1029/2011JD017293>.
- Tang, Q., Durand, M., Lettenmaier, D.P. and Hong, Y. (2010) Satellite-based observations of hydrological processes. *International Journal of Remote Sensing*, 31(14), 3661–3667. <https://doi.org/10.1080/01431161.2010.483496>.
- Tang, Q., Gao, H., Lu, H. and Lettenmaier, D.P. (2009) Remote sensing: hydrology. *Progress in Physical Geography*, 33(4), 490–509. <https://doi.org/10.1177/0309133309346650>.
- Taylor, K.E. (2001) Summarizing multiple aspects of model performance in a Single Diagram. *Journal of Geophysical Research*, 106(D7), 7183–7192. <https://doi.org/10.1029/2000JD900719>.
- Te, N. (2007) Drought management in the lower Mekong Basin. *Presentation at 3rd Southeast Asia water forum*. Kuala Lumpur, Malaysia. pp. 22–26.
- Torrence, C. and Compo, G.P. (1998) A practical guide to wavelet analysis. *Bulletin of the American Meteorological Society*, 79, 61–78.
- Wang, A. and Zeng, X. (2012) Evaluation of multireanalysis products with in situ observations over the Tibetan Plateau. *Journal of Geophysical Research Atmospheres*, 117(5), 1–12. <https://doi.org/10.1029/2011JD016553>.
- Wang, F., Ge, Q., Chen, D., Luterbacher, J., Tokarska, K.B., Hao, Z., Liu, Y. and Wu, M. (2018) Global and regional climate responses to national-committed emission reductions under the Paris Agreement. *Geografiska Annaler* (in press).
- Wang, W., Lu, H., Yang, D., Sothea, K., Jiao, Y., Gao, B., Peng, X. and Pang, Z. (2016) Modelling hydrologic processes in the Mekong River Basin using a distributed model driven by satellite precipitation and rain gauge observations. *PLoS One*, 11, e0152229.
- Whitcher, B., Guttorp, P. and Percival, D.B. (2000) Wavelet analysis of covariance with application to atmospheric time series. *Journal of Geophysical Research: Atmospheres*, 105(D11), 14941–14962.
- Wong, J.S., Razavi, S., Bonsal, B.R., Wheeler, H.S. and Asong, Z.E. (2017) Inter-comparison of daily precipitation products for large-scale hydro-climatic applications over Canada. *Hydrology and Earth System Sciences*, 21(4), 2163–2185. <https://doi.org/10.5194/hess-21-2163-2017>.
- Wu, F., Wang, X., Cai, Y. and Li, C. (2016) Spatiotemporal analysis of precipitation trends under climate change in the upper reach of Mekong River Basin. *Quaternary International*. Elsevier Ltd and INQUA, 392, 137–146. <https://doi.org/10.1016/j.quaint.2013.05.049>.
- Yamamoto, M.K., Ueno, K. and Nakamura, K. (2011) Comparison of satellite precipitation products with rain gauge data for the Khumb region, Nepal Himalayas. *Journal of the Meteorological Society of Japan*, 89(6), 597–610. <https://doi.org/10.2151/jmsj.2011-601>.
- Yano, J.I. and Jakubiak, B. (2016) Wavelet-based verification of the quantitative precipitation forecast. *Dynamics of Atmospheres and Oceans*, 74, 14–29. <https://doi.org/10.1016/j.dynatmoce.2016.02.001>.
- Yatagai, A., Arakawa, O., Kamiguchi, K. and Kawamoto, H. (2009) A 44-year daily gridded precipitation dataset for Asia. *Solaia*, 5, 3–6. <https://doi.org/10.2151/sola.2009>.
- Yatagai, A., Kamiguchi, K., Arakawa, O., Hamada, A., Yasutomi, N. and Kitoh, A. (2012) Aphrodite constructing a long-term daily gridded precipitation dataset for Asia based on a dense network of rain gauges. *Bulletin of the American Meteorological Society*, 93(9), 1401–1415. <https://doi.org/10.1175/BAMS-D-11-00122.1>.
- Zeng, H., Li, L. and Li, J. (2012) The evaluation of TRMM Multisatellite Precipitation Analysis (TMPA) in drought monitoring in the Lancang River Basin. *Journal of Geographical Sciences*, 22(2), 273–282. <https://doi.org/10.1007/s11442-012-0926-1>.
- Zhao, Y., Xie, Q., Lu, Y. and Hu, B. (2017) Hydrologic evaluation of TRMM multisatellite precipitation analysis for Nanliu River Basin in Humid Southwestern China. *Scientific Reports*, 7(1), 1–10 Springer US. <https://doi.org/10.1038/s41598-017-02704-1>.
- Zhou, T., Yu, R., Chen, H., Dai, A. and Pan, Y. (2008) Summer precipitation frequency, intensity, and diurnal cycle over China: a comparison of satellite data with rain gauge observations. *Journal of Climate*, 21(16), 3997–4010. <https://doi.org/10.1175/2008JCLI2028.1>.
- Ziv, G., Baran, E., Nam, S., Rodriguez-Iturbe, I. and Levin, S.A. (2012) Trading-off fish biodiversity, food security, and hydropower in the Mekong River Basin. *Proceedings of the National Academy of Sciences*, 109(15), 5609–5614. <https://doi.org/10.1073/pnas.1201423109>.

SUPPORTING INFORMATION

Additional supporting information may be found online in the Supporting Information section at the end of the article.

How to cite this article: Chen A, Chen D, Azorin-Molina C. Assessing reliability of precipitation data over the Mekong River Basin: A comparison of ground-based, satellite, and reanalysis datasets. *Int J Climatol*. 2018;38:4314–4334. <https://doi.org/10.1002/joc.5670>